

# Design and fabrication of thermoelectric generators into textile, with area selective ALD and spraying

Suvi Leppänen

**School of Chemical Technology**

*Thesis submitted for examination for degree of Master of Science in Technology.*

*Espoo, 27.5.2019*

**Supervisor**

*Professor Maarit Karppinen*

**Advisors**

*M.Sc. (Tech) Giovanni Marin and M.Sc. Fabian Krah*

---

**Author** Suvi Leppänen

---

**Title** Design and fabrication of thermoelectric generators into textile, with area selective ALD and spraying

---

**Master's programme in** Chemical, Biochemical and Materials Engineering

---

**Major** Functional materials**Code** CHEM3025

---

**Thesis supervisor** Professor Maarit Karppinen

---

**Thesis advisors** M.Sc. (Tech) Giovanni Marin and M.Sc. Fabian Krahel

---

**Date** 27.05.2019**Number of pages** 59**Language** English

---

---

**ABSTRACT**

---

Thermoelectric devices can utilize a temperature difference to produce electrical power in a scalable manner. This makes it a promising solution to power the growing demand for wearable electronics. Since the current state-of-the-art thermoelectric materials bismuth telluride ( $\text{Bi}_2\text{Te}_3$ ) and antimony telluride ( $\text{Sb}_2\text{Te}_3$ ) are brittle and toxic for humans, more research for wearable solutions and materials for fabric substrates is needed to reach this goal. The issues that need to be solved by research are to find appropriate flexible and nontoxic material solutions available, a reliable deposition method and a functional design for the direction of the temperature difference.

For a thermoelectric design to work impregnated into a textile substrate the placement and edges of the two deposited materials need special attention. The two different semiconductor materials cannot be in contact with each other but also need to be thick enough to overcome the electrical resistance of the fabric. Although, atomic layer deposition is a technique for precise pinhole free deposition, limiting deposited areas is a challenge, especially when depositing on a fabric substrate.

This thesis will attempt to design and fabricate a thermoelectric generator using zinc oxide and poly(3,4-ethylenedioxythiophene)poly(styrenesulfonate) by impregnating these materials into a fabric substrate. The impregnation will be done with area selective atomic layer deposition and spraying, to achieve the proposed design. A literature section has been outlined to describe the relative theory behind the design and the chosen materials for this work while the experimental section reviews the methods and results for fabricating the proposed design.

---

**Keywords :** Atomic layer deposition, Zinc oxide, PEDOT:PSS, Thermoelectric devices, textile

---

---

**Författare** Suvi Leppänen

---

**Titel** Tillverkning av en termoelektrisk generator på tyg med hjälp av begränsad atomlagerdeponering och sprutmålning

---

**Utbildningsprogram** Materialteknik

---

**Huvudämne** Funktionella material

**Huvudämnets kod** CHEM3025

---

**Övervakare** Professor Maarit Karppinen

---

**Handledare** DI Giovanni Marin och DI Fabian Krah

---

**Datum** 27.05.2019

**Sidantal** 59

**Språk** Engelska

---

## SAMMANDRAG

---

Termoelektriska enheter kan utnyttja en temperaturskillnad för att skapa elektricitet, tekniken är mekaniskt hållbar och den skapade spänningen är proportionell till temperaturskillnaden mellan de olika polerna. Detta gör termoelektricitet till en lovande lösning för att skapa trådlös el åt kroppsnära teknik, som är en växande teknikform på väg till marknaden. Dagens termoelektriska material ( $\text{Bi}_2\text{Te}_3$ ) är sköra och giftiga, så nya lösningar krävs för att utnyttja tekniken effektivt. Tyger som består av termoelektriska moduler bör vara utav flexibla och ogiftiga material som kan deponeras på ett kontrollerbart sätt till enligt riktningen av temperaturskillnaden.

För att ett termoelektriskt mönster skulle fungera impregnerat i tyg, är det viktigt att de olika deponerade materialen inte i kontakt med varandra och är i tillräckligt tjocka lager för att överkomma tygets elektriska resistans. Atomlagerdeponering är en deponerings teknik som är känd för att kunna deponera felfria tunnfilmer av material på en variation an underlag. Denna deponerings teknik kan också vara väldigt täckande, vilket kan göra begränsande av filmen svårt.

Denna avhandling tillverkar ett termoelektriskt mönster för att deponeras på tyg, där temperaturskillnaden kommer att vara längs med tyget. De termoelektriska materialen som mönstret består av är zinkoxid och en elektriskt ledande polymer (PEDOT:PSS). Mönstret fabriceras på ett bomull tyg substrat med hjälp av begränsad atomlagerdeponering för zinkoxid och begränsad sprutmålning av PEDOT:PSS. Avhandlingen är delad till en litteraturandel där nuvarande läget av forskningen är behandlad och en experimentell andel där fabricerings metoderna för mönstret är beskrivna.

---

**Nyckelord:** atomlagerdeponering, zinkoxid, PEDOT:PSS, termoelektriska enheter, textil

---

## PREFACE

---

The experimental work for this thesis was done at Laboratory of Inorganic Chemistry for the School of Chemical Engineering during the spring of 2019. I would like to thank my advisors Giovanni Marin and Fabian Krahle for continuous support and assistance throughout this project, even as things haven't always gone as planned. I am grateful to my supervisor Maarit Karppinen for providing me with this interesting thesis topic to work on. A special thanks to Aalto university workshop located in the Chemistry building for making the masks used in this thesis.

I would also like to thank my family and friends for their patience and support during my studies and the making of this thesis, especially Wäinö, without who's support this project might have become overwhelming.

Espoo, 27.5.2019

Suvi Leppänen

# TABLE OF CONTENTS

---

|  |     |
|--|-----|
| Abstract .....                               | i   |
| Sammandrag .....                             | ii  |
| Preface .....                                | iii |
| Table of Contents .....                      | iv  |
| Symbols and Abbreviations .....              | vi  |
| 1 Introduction .....                         | 1   |
| Literature Section.....                      | 3   |
| 2 Thermoelectric effect .....                | 3   |
| 3 Atomic Layer Deposition .....              | 9   |
| 3.1 Deposition methods.....                  | 12  |
| 3.2 Area Selective ALD .....                 | 15  |
| 4 Flexible thermoelectric leg materials..... | 17  |
| 4.1 P-type conductive polymer .....          | 17  |
| 4.2 N-type Zinc oxide.....                   | 19  |
| 5 Thermoelectric textiles.....               | 22  |
| Experimental section .....                   | 27  |
| 6 Goals for these experiments.....           | 27  |
| 7 Synthesis and characterisation .....       | 28  |
| 7.1 Making the samples .....                 | 28  |
| 7.1.1 Structure concept .....                | 29  |
| 7.1.2 Area Selective Spraying .....          | 33  |
| 7.1.3 Area Selective ALD.....                | 35  |
| 7.2 Thermoelectric effect .....              | 39  |

|     |  |    |
|-----|--|----|
| 8   | Results .....                          | 41 |
| 8.1 | Selectively deposited PEDOT:PSS.....   | 41 |
| 8.2 | Selectively deposited Zinc Oxide ..... | 44 |
| 8.3 | Thermoelectric characteristics .....   | 49 |
| 9   | Conclusions and discussion .....       | 52 |
|     | References .....                       | 54 |

## SYMBOLS AND ABBREVIATIONS

---

### Symbols

|             |  |
|-------------|--|
| $S$         | <i>Seebeck coefficient</i>                   |
| $\sigma$    | <i>electrical conductivity of a material</i> |
| $\kappa$    | <i>thermal conductivity of a material</i>    |
| $\kappa_e$  | <i>electrical thermal conductivity</i>       |
| $\kappa_l$  | <i>lattice thermal conductivity</i>          |
| $S^2\sigma$ | <i>thermoelectric power factor</i>           |
| $\Omega$    | <i>electrical resistance (Ohm)</i>           |

### Abbreviations

|           |   |
|-----------|---|
| ALD       | Atomic Layer Deposition                                 |
| ALE       | Atomic Layer Epitaxy                                    |
| AZO       | Aluminium doped Zinc Oxide                              |
| CVD       | Chemical Vapor Deposition                               |
| DEZ       | Diethyl Zinc  |
| MLD       | Molecular Layer Deposition                              |
| PE-ALD    | Plasma enhanced ALD                                     |
| PEDOT     | Poly(3,4-ethylenedioxythiophene)                        |
| PEDOT:PSS | Poly(3,4-ethylenedioxythiophene) poly(styrenesulfonate) |
| PGEC      | Phonon-Glass/Electron Crystal                           |
| SAM       | Self-Assembled Monolayers                               |
| TE        | Thermoelectric effect                                   |
| TEG       | Thermoelectric generator                                |
| TH-ALD    | Thermal ALD   |
| TMA       | Trimethyl Aluminium                                     |
| VDP       | Vapor Deposition Polymerization                         |
| ZT        | Thermoelectric figure of merit                          |

# 1 INTRODUCTION

---

Wearable electronics have become an increasingly popular concept due to the possibility of directly integrating wearable sensors and healthcare devices [1] into the fabric. Therefore, a need has emerged for a wireless power source. While there are many solutions to generate large amounts of power at a time, it can be challenging to distribute the electricity in micro ( $> 10 \mu\text{W}$ ) amounts. A suitable solution could be to use thermoelectric devices, as this technology can convert heat gradients to electricity without any need for external solutions such as charging. Thermoelectric devices can be lightweight, quiet and long-lasting if done correctly, as it has no moving parts. [2]

In recent years, much research has been devoted to making thermoelectric textiles a reality. This has involved finding the suitable thermoelectric materials for different applications [3], testing the effect that different fabrics can have on conducting electricity[4], designing a functional generator [5] as well as understanding the limitations involved [6]. However, all of these textile and design solutions have focused on only one type of flexible thermoelectric material, while a more effective solution would be to use two different types of flexible materials (n-type and p-type) for an efficient flow of current.

Currently, the state-of-the-art room-temperature materials used in thermoelectric devices are ceramics, most of these are also rigid, toxic and expensive [7]. Therefore, new innovative and flexible material solutions are needed for fabric substrates. Zinc oxide (ZnO) shows great potential as a well-researched material that could be used as a thermoelectric n-type material, since it can create transparent thin films and is nontoxic [8]. For a p-type material, conductive polymers offer some great alternatives for flexible thermoelectric devices. The state-of-the-art conductive polymer with thermoelectric properties is Poly(3,4-ethylenedioxythiophene) poly(styrenesulfonate) (PEDOT:PSS)[9].

In order to ensure a functional design, the two thermoelectric material types (also called legs) must not come into contact with each other. However, fabric differs from other substrates in that thin films cannot be reliably removed from it after deposition. The



deposition techniques must therefore be area selective, precise, and the fabrication must occur in distinguished steps. Other the major contributing factors to the design are how to connect the different thermoelectric materials as well as keeping in mind the in which direction the heat difference will be and designing accordingly.

The aim of this thesis is to develop a functioning design for selectively depositing a two-legged (p- and n-type) thermoelectric generator into a fabric substrate, as well as to evaluate the performance of the proposed design. The proposed design will be deposited on Silicon oxide and cotton substrates. The legs will be composed of ZnO and PEDOT:PSS, which will be selectively deposited using ALD and spraying, respectively. While many solutions for optimizing thermoelectric materials are available, this thesis will not utilize these possibilities due to time constraints.

The literature section describes the thermoelectric effect, its underlying theory as well as the materials and deposition techniques that can be used to fabricate a thermoelectric fabric. Chapter 2 goes into details in the requirements for fabricating a thermoelectric device. Chapter 3 introduces the atomic layer deposition (ALD) technique, and area selective ALD, which is a focus of this thesis. Chapter 4 reviews the thermoelectric materials used in this work. To draw all these different elements together, Chapter 5 summarizes the combination of all these factors in terms of the textile substrate. The experimental section will provide an overlook on the goals of the experiment in Chapter 6, as well as the methods and results of the experiments in Chapter 7 and 8, respectively.

## LITERATURE SECTION

### 2 THERMOELECTRIC EFFECT

In 1821, the German physicist Thomas Johann Seebeck noticed that a compass needle deflected when it was brought near two connected dissimilar metals that were at different temperatures. The effect was later discovered to be caused by an electric current between the differently heated metals and named “thermoelectricity”, also known today as the Seebeck effect. The Seebeck coefficient ( $S$ ) is defined by the voltage developing from a thermal difference ( $\Delta T$ ) between the measured voltage points,  $S = \Delta V / \Delta T$ . The Seebeck coefficient can be either positive or negative, depending on the dominant charge carrier. A material with a negative Seebeck coefficient is an n-type material, while a p-type material has a positive Seebeck coefficient.[10] The opposite of the Seebeck effect is called the Peltier effect, which uses a power for cooling. When a current is added to a system of two dissimilar materials, heat is collected from outside the material to compensate for the added current.[11]. Both effects are applicable in thermoelectric solutions, as illustrated in Figure 1.

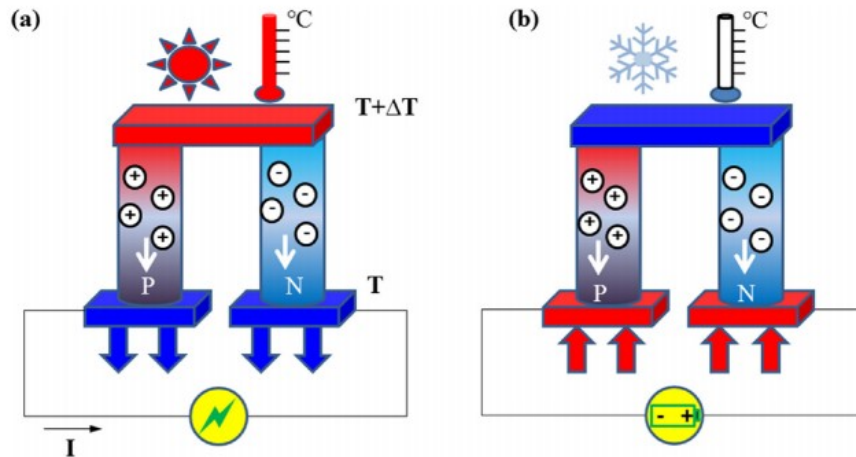


Figure 1. Illustrations of a thermoelectric module, a) shows the Seebeck effect and b) shows the Peltier effect. [12]

For thermoelectric modules to generate power, there needs to be a temperature gradient between the two poles of the device. Increasing the temperature difference increases the

power generation. In general, thermoelectric generators have a low heat-to-electricity conversion efficiency. With the state-of-the-art materials today, an experimental efficiency of 5% can be obtained at high temperatures when the goal is 20%. The efficiency decreases even more with decreasing temperature differences. [13]

The efficiency of thermoelectric effect (TE) is measured with a figure of merit  $ZT$ . The value of  $ZT$  describes the efficiency of the material as a thermoelectric component. The figure of merit is defined by the following formula:

$$ZT = \frac{S^2 \sigma}{\kappa} T \quad (1)$$

where  $S$  represents Seebeck coefficient,  $\sigma$  the electrical conductivity,  $\kappa$  the thermal conductivity and  $T$  the temperature dependency. A specific  $ZT$  value can only be achieved at specific temperatures. Since thermal conductivity can vary depending on the type of conductivity, a more specific clarification for  $\kappa$  is  $\kappa = \kappa_e + \kappa_l$ , where  $\kappa_e$  denotes the electrical component and  $\kappa_l$  the lattice component of thermal conductivity. [11] The sought after  $ZT$  value of  $\geq 3$  is yet to be achieved with modern materials, though it would be desirable to achieve an even higher value. Although  $ZT$  has no theoretical maximum limit, the best bulk materials have only a practical  $ZT$  value of about 1. [14]

Achieving a good figure of merit for a thermoelectric material is difficult due to the complex nature of the material properties. For an efficient power factor ( $S^2\sigma$ ), both a high electrical conductivity ( $\sigma$ ) and a high Seebeck coefficient is desired, but as these two parameters conflict, the compromise lies somewhere in between when the carrier concentration is around  $10^{19}$ - $10^{20}$  carriers per  $\text{cm}^3$ . Usually, these properties can be found in heavily doped materials that have carrier concentrations somewhere between those of metals and semiconductors. In addition, reducing the electrical conductivity component ( $\kappa_e$ ) of the thermal conductivity will also inversely affect the actual electrical conductivity. [14]

Today, most efforts concentrate on lowering the lattice component ( $\kappa_l$ ) of thermal conductivity, as does not affect other coefficients [14]. Figure 2 shows a schematic of how the different components for the figure of merit relate to each other with respect of the

carrier concentration. Material properties are often dependent on each other, making finding the ideal material challenging. [3]

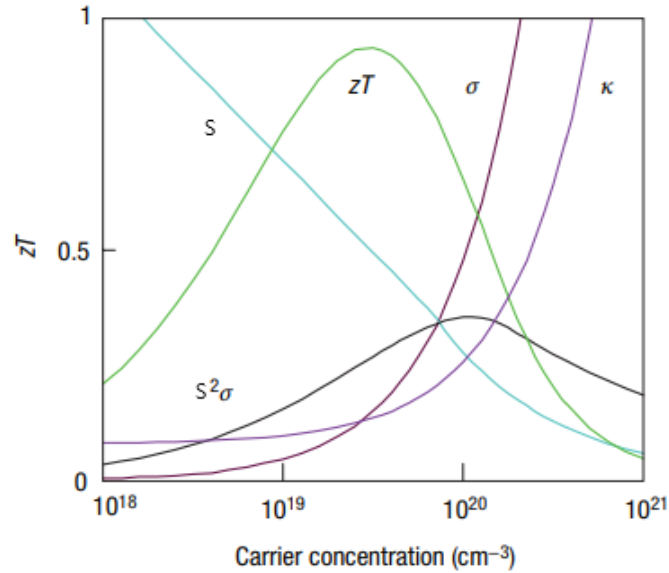


Figure 2. Maximizing the figure of merit in terms of the carrier concentration. Edited from source [3].

Currently, the most commercially used materials for thermoelectric are alloys of bismuth telluride ( $\text{Bi}_2\text{Te}_3$ ) and antimony telluride ( $\text{Sb}_2\text{Te}_3$ ). At low-temperature applications ( $> 200$  °C),  $\text{Bi}_2\text{Te}_3$  has the highest figure of merit in practical applications.  $\text{Bi}_2\text{Te}_3$  can be used as a both p-type and n-type of material. The best recorded ZT values for these materials range between 0.8-1.1, depending on the temperature and carrier concentration. For high-temperature applications ( $< 600$  °C), the most commonly used thermoelectric materials are alloys of silicon-germanium (SiGe), for both n- and p-type solutions. [3]

Thermoelectric materials are optimized when a narrow-bandgap semiconductor has a high mobility of carriers and the lattice thermal conductivity ( $\kappa_l$ ) is as low as possible. A suggested ideal thermoelectric material would be a “Phonon-Glass/ElectronCrystal” (PGEC) where thermal properties would be such as that of glass and electrical properties similar to that of a single crystal material. [15]

Most currently researched thermoelectric are composed of a complex structure. Among the complex structures researched include Chalcogenide, Half-Heusler, Skutterudite,

Silicide, and Oxide materials. The different structures have shown great potential as thermoelectric materials for varying reasons. Adding nanostructures to a material has shown improvement in the thermoelectric figure of merit for that material. Nanostructuring can reduce the thermal lattice conductivity by making the available material more complex. [11]

Thermoelectric modules normally consist of two different types of material for utilizing the carrier concentration to the fullest. The different modules are usually connected in series. Thermoelectric generators can be constructed of only one type of material, but this is less efficient and creates some issues in how the materials are to be connected. Figure 3 shows the different ways to connect modules to produce electricity. [16] While using two different carrier types in a module lowers the Seebeck coefficient, it is beneficial as the charge is moving with two types of carrier types, thereby cancelling out the Seebeck voltages [3].

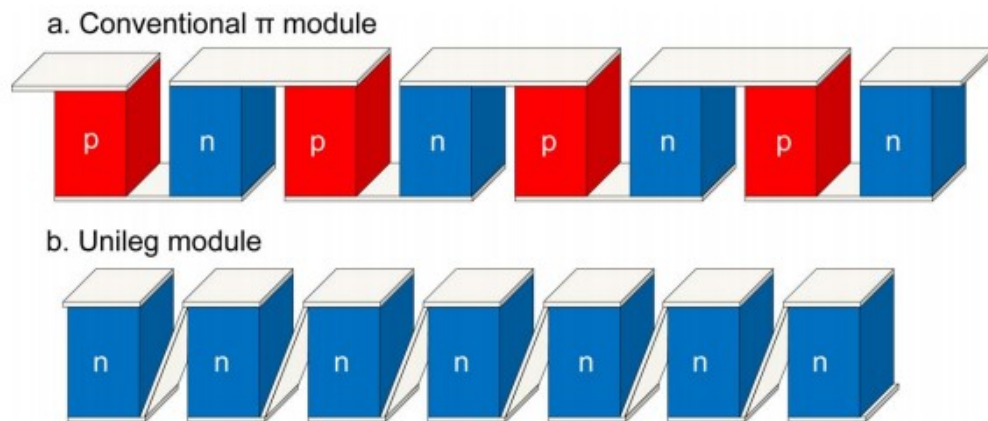


Figure 3. Thermoelectric modules a) typical two type material module and b) one type material module.

[16]

The structure of a thermoelectric generator (TEG) usually consists of several modules that are connected electrically in a series and thermally parallel. This type of construction makes it possible to build thermoelectric generators in varying sizes, as the structure is

scalable. It is also mechanically robust, as it has few moving parts, thus reducing the need for maintenance. [3]

Bulk thermoelectric devices are three dimensional devices where the temperature difference penetrates through the thickness of the device. The thickness can be adjusted in order to control more easily the temperature gradient between the poles. These devices are more rigid and more difficult to adjust to small scale use. This is where thin film thermoelectric modules become handy, as they are flexible and light making them applicable to almost any surface. In thin film TE devices, the thermoelectric charge normally travels through the plane instead of the thickness, as the thickness is low, and the temperature equalizes quickly. Figure 4 shows the different directions of heat in bulk and thin film thermoelectric generators. [17]

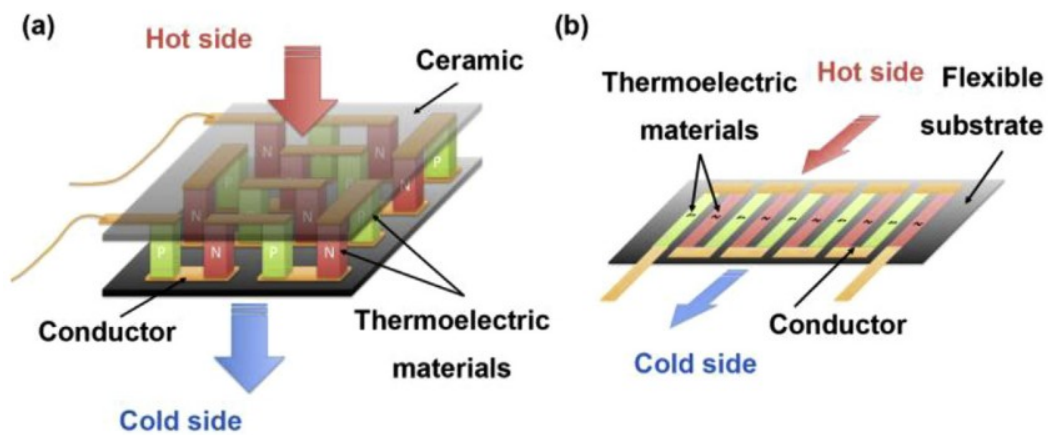


*Figure 4. Thermoelectric generators in a) bulk structure where heat travels through and b) thin film generators where heat travels in the plane direction. [17]*

Few studies have examined the effects of the substrate in thin film thermoelectric generators. Nevertheless, one study by Marin et al. [5] coated where thermoelectric material on three different substrates. They found that the substrate used affects the thermoelectric device performance. Especially the thickness and thermal conductivity of the substrate were found to be contributing factors, with the thinnest substrate

performing the best even though it did not have the best thermal conductivity of the tested substrates.

### 3 ATOMIC LAYER DEPOSITION

---

Atomic layer deposition (ALD) is a chemical vapor deposition (CVD) method to produce thin films on varying substrates with great precision. The technology has become a standard in the semiconductor industry due to the ever-increasing need for miniaturization of computers. The high standard for uniformity and detail for semiconductor thin films cannot be achieved by any other deposition technique. [18]

Atomic layer deposition was developed by Tuomo Suntola in the 1970s in Finland. At that time, it was named Atomic layer epitaxy (ALE) and was known with that name until the end of the century. It was first used to produce electroluminescent displays but was found to be applicable to many other production needs as well. [18]

Growing thin films using ALD works in sequential steps by first introducing the substrate to a gas phase precursor that reacts on the substrate to form a uniform layer on the substrate, this is the first pulse. Between every pulse in a cycle, a purge is performed with the help of an inert carrier gas that removes all the excess material from the reaction chamber. The second pulse consists of another precursor material that reacts chemically with the first, producing the desired atomic layer. After the second purge, the first cycle is finished. [19] An illustration of this cycle and its steps can be observed in Figure 5. By controlling the number of deposition-cycles a specific layer thickness can be achieved. The different reactions are self-limiting, resulting in conformal layers that can be deposited on various substrates with varying texture and size. [20]

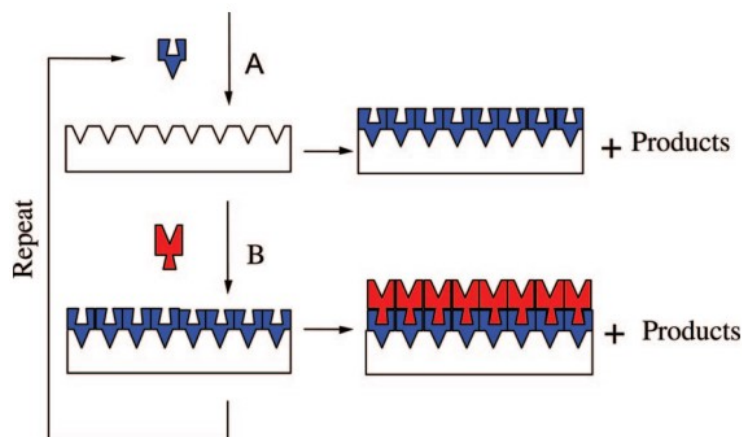


Figure 5. Schematic representation of an ALD cycle, where A and B are the precursors. [18]



Atomic layer deposition has several benefits compared to other similar deposition methods. The self-limiting manner ensures that only a specific amount of matter is used. With the right conditions the amount of cycles determines the thickness of the deposited layer. Compared with traditional chemical vapor deposition techniques the flux does not influence the reaction too much, as all the excess matter is purged from the reactor. These aspects make it possible to get a uniform coating on large areas and makes the process easily repeatable. With ALD it also possible to create complex layered structures with different materials in layers to achieve specific properties in the combined material. [21]

Most ALD reactors utilize a vacuum in the reaction chamber to eliminate contaminants and side reactions during deposition. The temperature in the reaction chamber defines if the surface chemistry to yield the deposition takes place at all and how efficient the reaction is. [17] When the temperature of the reaction is lower than needed it results in slow reaction kinetics or that the precursor might condensate. At too high temperatures the precursor might decompose thermally or desorb rapidly which will lead to poor growth rates and unwanted deposition formations. [22]

The main limitation of ALD is considered to be its low growth rate. A typical deposition speed is about 100 nm/h thickness on a substrate, but as this can be done on several or large substrates simultaneously. ALD is still is a reasonable thin film deposition technique due to its even layers. The chemically suitable materials to use with ALD are also limited, while there are more applicable materials found all the time there will probably never be quite enough to suit industrial needs. To reach proper uniformity there is an issue also with impurities that easily enter the reaction with the substrate, these can affect the resulting film. [23]

Atomic layer deposition is always managed in a reactor. There are several reactor types that are composed of slightly different setups for slightly different effects. Most reactors in industry and laboratories are flow-type reactors, because the different steps of the cycle can be achieved in a fast and reliable way. [20] Depending on the reactor and the different materials, one cycle can take from a fraction of a second to a couple of seconds and produce a layer with a thickness of 0,1 to 3 Å. [19]

A flow type reactor works usually in a vacuum pressure of about 1 Torr, these can be categorized by either viscous flow or transition flow conditions [20]. The defining feature is how the precursors enter and leave the reactor with the help of an inert carrier gas that is also used for purging the reactor. Viscous flow type reactors work with a viscous continuous flow of carrier, that also carries the precursor material to and out of the chamber. The precursors only have a short time to react in the chamber making the depositing faster but also the reaction harder to predict. [18] Figure 6 displays the process and instrumentation diagram of a continuous cross-flow type reactor [24].

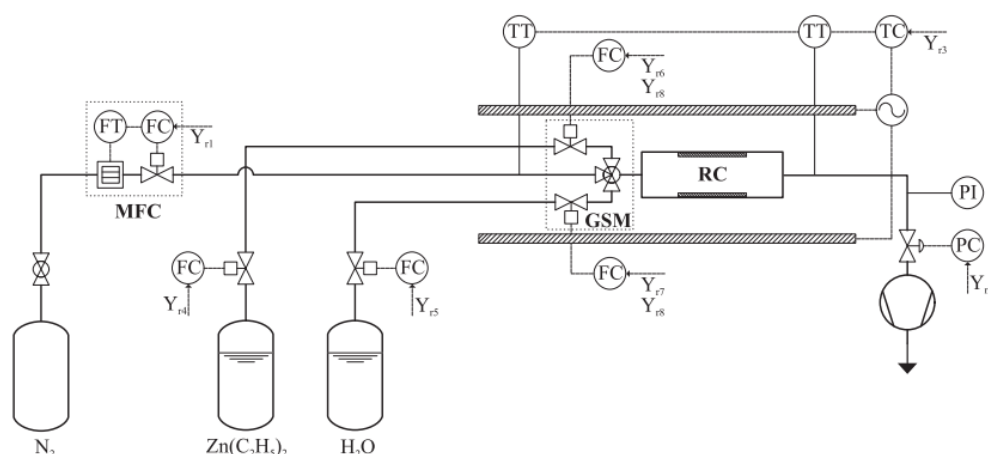


Figure 6. Continuous flow ALD reactor schematic [24]

One of the main ingredients of a successful ALD is combining the right precursors. There are many materials that can be used as precursors, in a gaseous, volatile liquid or solid form. For effective transportation, the vapor pressure needs to be high enough for mass transportation, and some liquids and most solids need to be heated before use. Another requirement of the precursors is that the precursors must be thermally stable at the growth temperature, any decomposition during a reaction would compromise the self-limiting reaction. [19]

All precursors must be self-terminating in the gas to solid reactions. These precursors can be divided in to two main categories; inorganic and metalorganic. The simplest precursor

is an elemental form precursor that can react with both elemental non-metals and hydrogen compounds. The benefit of simple elements as precursor is the lack of extra ligands that could cause hindrances in the reaction. [25]

When depositing oxide thin films, it is important to keep in mind that the substrate must have active surface hydroxyl groups to enable the precursor to have a chemical reaction with. The hydroxyl groups (x-OH) acts as an anchor for the metal vapor as it reacts with the surface. These can also be used to react with a water precursor, which is common with oxide reactions, to leave the oxide of the water behind on the substrate as the water precursor is removed. [26]

### 3.1 DEPOSITION METHODS

There are many different types of ALD available, but the categories can be defined in many ways depending on the chemistry, parameters or product. In this work, the ALD methods are categorized according to temperature and resulting layer material, with special emphasis on low-temperature solutions.

High-temperature ALD, or what consider as the conventional ALD is mostly driven by the thermal energy in the reactor to complete the reaction. Most thermal ALD (TH-ALD) recipes have been adaptations of the older binary CVD techniques but instead of having all reactants in the chamber at the same time, having them added one at a time in sequences. These reactions require a temperature of 100-600 °C to produce a decent layer per cycle, as the reaction requires to heat the resulting bond is stronger. Most of these reactions produce binary products such as metal oxides, metal nitrides or sulphides. [18]

Not all substrates can tolerate the high temperatures of typical ALD, this led to finding solutions for a reliable ALD even in lower temperatures. This is especially a problem for the need of nanostructuring which is beneficial among others in thermoelectric materials. Fortunately, several thermal approaches work even in lower temperatures and in special cases, a catalyst can be added. Many of these binary depositions the reaction enthalpy is

negative, resulting in robust reactions even in low temperatures, for example  $\text{TiO}_2$  and  $\text{ZnO}$  have reaction enthalpies of -16 and -70 respectively. [18]

With thermal ALD, the common secondary precursor of  $\text{H}_2\text{O}$  can cause issues at higher temperatures as the precursor might cause unwanted oxidation. Partially, as it can stick to a surface without being purged. This can cause mechanical or electrical issues in the substrate. The other common oxidizing precursor  $\text{O}_3$  can also cause reduced electrical properties, while it can be more effectively used in lower temperatures. [27]

Plasma enhanced ALD (PE-ALD) can give more process flexibility by potentially increasing the deposition quality and enabling lower substrate temperature solutions. This is possible by reducing the need to use  $\text{H}_2\text{O}$  as a precursor material and instead use  $\text{O}_2$  or  $\text{O}_3$  plasmas as oxidants. PE-ALD can be divided into three different categories. First is direct plasma ALD, where the electrode to create plasma works as the substrate holder. Second is remote plasma ALD, where the plasma is created separately from the substrate and later brought together. The third category is radical enhanced ALD, where the electrons from the plasma never come in to contact with the substrate. [28]

Metal ALD is problematic, most trials to deposit pure metals using CVD chemistry have failed. This is thought to be due to a lack of reactive sites for metal to be deposited on the metal. The use of radicals or hydrogen-plasma-enhanced ALD has helped to produce successful ALD with good results. The reaction is assisted by the radicals in the plasma when the heat is not enough to induce the process [18]. Figure 7 shows an ALD cycle with the help of radical exposure. Copper remains as one of the most difficult metals to successfully deposit with ALD, some successes have been to deposit  $\text{CuO}$  on a surface and later reduce the thin film to metallic copper with separate treatments. [19]

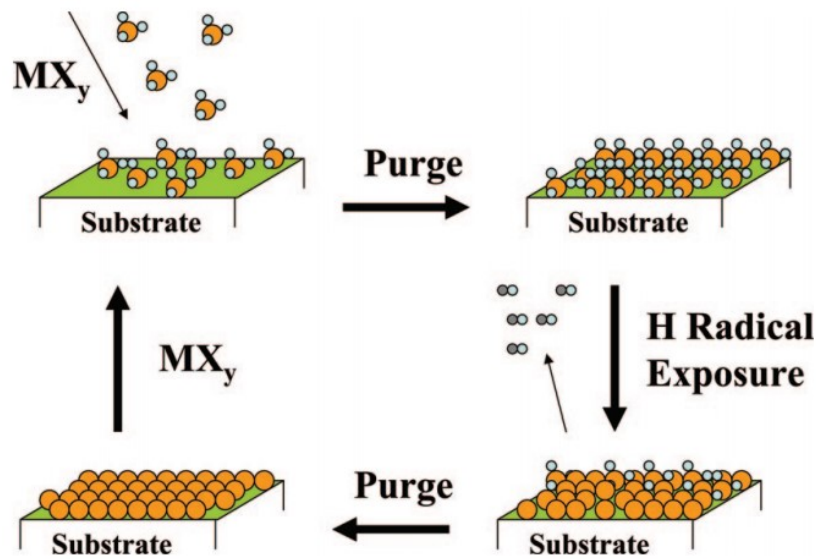


Figure 7. Radical enhanced ALD cycle [18].

Most ALD produces inorganic binary thin films, to overcome this limitation a similar production method was developed called Molecular Layer Deposition (MLD). In MLD the process one or both precursors are organic molecules, sometimes they contain inorganic constituents. The deposition works by stepwise condensation of polymers. Similar to that of ALD, it is related to chemical vapor deposition, MLD is a vapor deposition polymerization (VDP) technique that uses gas-phase polymer-growth. This produces pinhole free organic thin films. The challenges with MLD come from a need for low-temperature solutions due to the organic materials and the problematic nature of organic material when it comes to vapor pressure and gas-phase chemistry. [29]

As the two deposition types are very close to each other, a hybrid deposition technique MLD/ALD is developed where both inorganic and organic materials can be combined to produce a hybrid thin film. The idea is to create a method to produce new types of superlattice and nanolaminate structures when the deposition control approaches that of conventional ALD. But combining the two deposition types is not as straightforward as it seems. [30]

### 3.2 AREA SELECTIVE ALD

ALD normally deposits the thin film on the entire substrate, since it is a vapor deposition technique it is harder to limit growth on areas where deposition is not wanted. If it is possible to choose the area where the deposition occurs a whole new level of possibilities in ALD become available. To select the deposition areas there needs to be a mask or chemical way to protect the substrate from being fully deposited. The previous ways of selecting the resulting thin film have been done with the help of etching, where the unwanted depositions are removed chemically after deposition. This is a very time-consuming solution and is not workable on all substrates, making Area Selective Atomic Layer Deposition a necessary research area. [31]

There are some approaches to area selective ALD where they use reactive compounds as surface modifying agents to limit the reactive sites on the substrate. Especially the use of Self-Assembled Monolayers (SAMs) have shown success to block precursor nucleation in the unwanted areas when depositing inorganic metal oxide films. The tests only worked when the SAM film has been pinhole free to control the nucleation sites, which is extremely difficult to make. Making it an ineffective and unreliable way to get industrial support. [32]

In ALD reactants can penetrate and reach areas between a mask and substrate if the areas are not properly sealed, this is especially true if the substrate has a high surface area or is porous. However, if the substrate is thin and soft in nature, it can be pressed between masks to reduce the lateral movement of the precursor in between the masks. The spreading of the precursor in the substrate can then be controlled by adjusting precursor dosing times, number of cycles and deposition temperature with various success. Figure 8 illustrates the masking concept in comparison with regular ALD on a nonwoven textile substrate. [33]

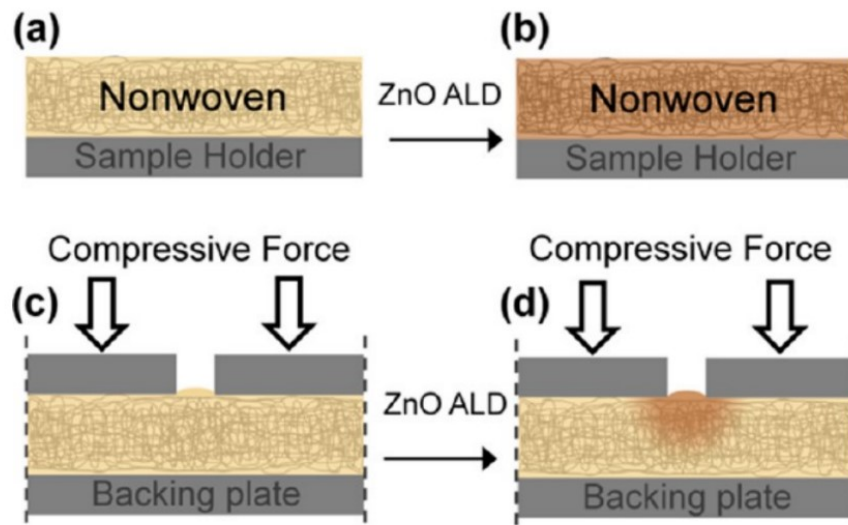


Figure 8. Mechanical force masks for patterning ALD (c & d) in comparison with regular ALD (a & b).[33]

Researchers have defined area selective deposition methods according to the mechanisms of the mask, the categories are defined as “inherent”, “activated” and “passivated”. The “inherent” selectiveness implies a clean patterned surface where the pattern slows down the nucleation in comparison with open growth areas. This has yielded satisfactory results. The “Activated” method uses an external energy source to imprint certain areas for growth by using phonons, electrons, and ions among others. When a specific area is “Passivated” it implies that certain areas have specifically chemically masked, so that the masked areas do not react with the precursor materials. Passivation has been proven to work, but also add more steps into the process making optimization difficult. [34]

The key problems in area selective depositions according to Parsons [34] are,

- How much material can be deposited before deposition occurs in unwanted areas?
- Do the quality and effectiveness translate when using masked substrates?
- Which mechanism causes unwanted growth so overall performance can be improved?

Due to the fabric substrate used in this thesis, a solid aluminium mask will be used to limit ALD growth on the textile. Chemical approaches would be harder to remove completely from textile as it can absorb substances deep in to the fibre.

## 4 FLEXIBLE THERMOELECTRIC LEG MATERIALS

---

The flexible thermoelectric materials used to produce the thermoelectric modules on different substrates in this work, are presented in the following sections. These subchapters present how these materials work, their properties and the way they can be deposited on substrates.

### 4.1 P-TYPE CONDUCTIVE POLYMER

Polymers are lightweight and flexible, they can also be made conducting making them a promising new solution for thermoelectric devices. Polymers can also be easily distributed on different kinds of surfaces and topologies without losing the conductive nature of the material. As a lightweight material for thermoelectric use, it can be used on almost any surface or substrate that can tolerate contact with heat. [35]

The most common conductive polymer for thermoelectric use today is Poly(3,4-ethylenedioxythiophene) poly(styrenesulfonate) (PEDOT:PSS). The base material Poly(3,4-ethylenedioxythiophene) (PEDOT) is a conductive polymer, that has good semiconductor properties. PEDOT:PSS is a compound based on PEDOT that is electrostatically bound to polystyrene sulphonic acid (PSS). [36] PSS polyanion is added to make the polymer more convenient to use as the mix becomes soluble to an aqueous form [37].

PEDOT:PSS shows great potential and like most conductive polymers it has a lower thermal conductivity than most other inorganic thermoelectric materials, while having a decent electrical conductivity. Polymers still have a lower Seebeck coefficient than most other typical TE materials, showing that there is still improvement to be made. The highest reported power factor ( $S^2\sigma$ ) for a PEDOT:PSS thin film of a thickness of about 100 nm is about 30  $\mu\text{W mK}^{-2}$ . [38] The current best available ZT value for simple PEDOT that has been optimized with oxidation levels is  $ZT = 0,25$  at room temperature [39]. With optimization the ZT value of PEDOT:PSS with added 3 % Ethylene glycol the achieved value was  $ZT=0.27$  at room temperature, which is better than PEDOT on its own [40].



PEDOT:PSS has a positive Seebeck coefficient making it a typical p-type material for thermoelectric solutions. The positive charges carried by PEDOT are usually counterions. These counterions are called dopants, they cannot oxidize PEDOT even though the doping process is an oxidation reaction. There are different commercially available versions of the product, the most conducting version is PH1000 with an electrical conductivity up to 1000 S/cm. [41]

The reported ZT values vary in the literature, this can be due to the conditions and modifications to the material. All the properties of PEDOT:PSS is dependent of the ratio of PEDOT to PSS and the particle size of the dispersions in water. There are several additives that change the properties as it dries by rearranging the morphology of the particles, for example by adding a high boiling point solvent the electrical conductivity is increased. The arrangement and size of the different conducting PEDOT cores and insulating PSS shells in the dried thin film give different results.[42] The humidity of the area when the measurement is taken might also affect the results [41]. The general understanding of the composition is that when drying the spherical gel particles bond and create a solid film as seen in Figure 9A. Hydrogen bonds develop between the PSS rich outer shells promoting adhesion between the individual shells that form the thin film, this is shown in Figure 9B. [43]

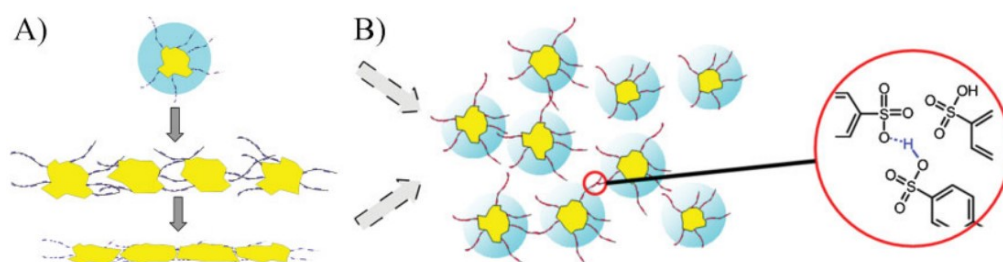


Figure 9. Illustration of PEDOT:PSS thin film formation mechanisms.[43]

The highly sought out feature of conductive polymers is the durability even through stretch and strain most these materials can keep some of their conductivity.

Vosgueritchian et al [44] tested that a four-layer film of PEDOT:PSS with 1 wt% fluorosurfactant Zonyl-FS300 could withstand stretching up to 10% for 5000 times without significant damage to the film. This is especially handy when depositing PEDOT:PSS on fabric and other textiles which are further investigated in Chapter 5.

PEDOT:PSS is mostly quite simple material to deposit on various substrates, as it comes in liquid form and dries relatively fast in air. The material has been sprayed, soaked in, or painted on a substrate. The easy processability of PEDOT:PSS makes it an ideal solution for thermoelectric applications. [45] Deposition on hydrophobic surfaces can be problematic but can be eased with fluorosurfactants [44].

## 4.2 N-TYPE ZINC OXIDE

Zinc oxide (ZnO) has a variety of potential uses in both bulk and thin film form. ZnO can be used as a piezoelectric material, a transparent electrode material for solar cells and gas sensors, and as a thermoelectric material, among others [46]. This chapter will focus on n-type Zinc Oxide-based materials for their thermoelectric properties and uses.

ZnO is generally known as a semiconductor material, that can be used as an n-type thermoelectric material. It is used due to its many useful properties and applications, but also because Zinc is relatively cheap material and it is nontoxic. ZnO has a wide band gap of 3.5 eV and a high decomposition temperature of 2200 K which makes it tolerate high temperatures without losing stability [47][48][49] (Ong, Singh et al. 2011) ZnO also has excellent charge carrier transport properties. Most of these properties can be greatly tuned with the help of doping. [50] It is also transparent giving it great potential in optic applications, including a high exciton binding energy of 60 meV [51]. ZnO can also be deposited in a variety of different ways making it an easy material to work with [52].

While ZnO on its own has a relatively high lattice thermal conductivity ( $\kappa_l$ ) which is not helpful for the overall ZT value, doping with aluminium has shown to improve these properties so that the doped material can have a ZT value of 0.3 at 1000 K [53]. This can

be further improved by nanostructuring the Al-doped ZnO (AZO) to a theoretical ZT value of 0.44 at 1000 K [50]. Currently the low temperature applications are not as convenient with doped ZnO resulting only in ZT values of less than 0.1 in room temperature [8].

Aluminium doping is proven to decrease the size of ZnO nanocrystals and increase their aspect ratios [50]. This improves the potential of the bulk material to some extent as can be seen in the high-temperature figure of merit calculation in Figure 10. According to the calculations the doping levels needed must stay around  $n \approx 2 \times 10^{19} \text{ cm}^{-3}$  to have a positive effect. These calculations do not take nanostructuring to account and the calculations concern bulk products. [49]

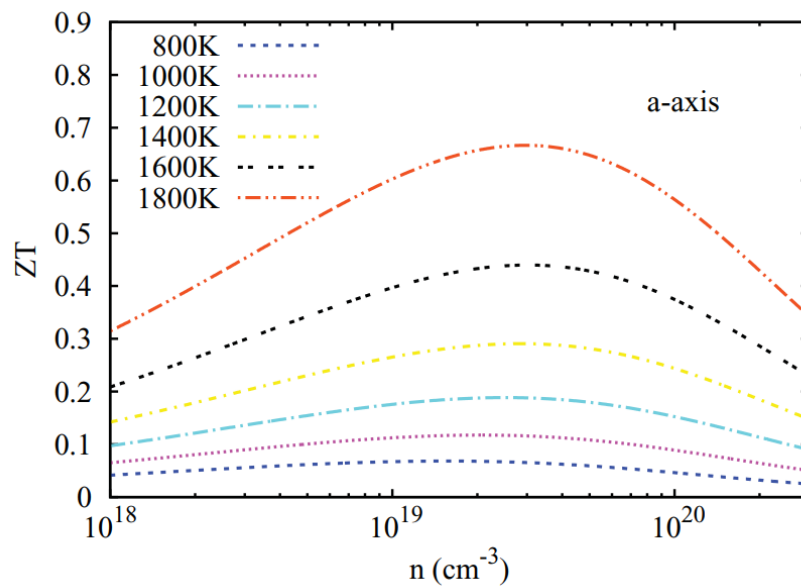
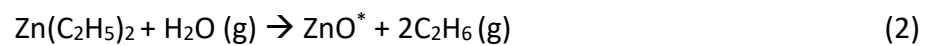


Figure 10. Calculated bulk zinc oxide ZT values with the effect of doping [49].

Zinc Oxide crystallizes in the hexagonal wurtzite structure that naturally exhibits n-type conductivity due to random defects that occur during synthesis. The exact reason for these impurities is not known which makes it hard to synthesize a p-type material of ZnO. Making p-type materials is possible but they are not easily reproduced or very durable, which makes it harder to only utilize ZnO in p-n junctions. [52] The nanodefects are different

from the synthesis in different temperatures making the ZnO resulting in varying properties. It is important to make sure that these defects are in equilibrium before exposing them to the rigorous heating and cooling typical for thermoelectric materials. [48]

Atomic layer deposition of ZnO has several different precursor solutions depending on the deposition temperatures and growth rate. The most common precursor to produce ZnO thin films is diethyl zinc (DEZ) which is usually used in a combination with water as the second precursor. The reaction can occur from room temperature up to 600 °C, where the typical deposition temperatures are in the range of 100-200 °C. This reaction is exothermic which allows for lower deposition temperatures than most other solutions. The reaction occurs according to the following mechanism [52]:



## 5 THERMOELECTRIC TEXTILES

---

Wearable electronics are becoming increasingly popular, with conductive textiles and fabrics many opportunities become available. Adding to that, when the electricity needs of our gadgets would be provided by our own bodies, there is opportunities like personalized health monitors with the help of self-powered sensors. [54] To enable this, the textile would need to be lightweight, comfortable and easy to care for in order to be functional, this rules out most bulk TEG solutions. With the help of thin film integrated textiles, that exhibit similar properties to that of normal fabrics this could be reality. [45]

This work will define textile as a networked composition of natural or artificial fibres, a focus on the naturally occurring fibres such as cotton. Natural fibres tolerate higher temperatures without deformation and come from renewable sources as well as being mechanically resilient. [4] Words such as textile and fabric will be used interchangeably in this text, referring to textile as a flexible fibre-based substrate.

Fabric is very versatile and widely used material with benefits such as flexibility and lightweight. Table 1 shows the mechanical properties of known textiles. As a thermoelectric substrate it provides also other benefits such as a low thermal conductivity so that it can take a while for the temperature to equalize through the substrate allowing for larger temperature differences between different ends of the substrate.[6] As a substrate it is also versatile as it can be built from scratch with different types of yarn to build a thermoelectric generator or coated with material for a similar effect. [54]

Table 1. Mechanical properties of known textiles [54].

| fibre  | initial modulus<br>(cN/tex) | yield stress<br>(cN/<br>tex) | tenacity<br>(cN/tex) | yield strain<br>(%) | strain at<br>break<br>(%) |
|--|-----------------------------|------------------------------|----------------------|---------------------|---------------------------|
| cotton   | 60                          | <sup>a</sup>                 | 40                   | <sup>a</sup>        | 7                         |
| wool   | 23                          | 6                            | 11                   | 5                   | 42                        |
| silk   | 73                          | 16                           | 38                   | 3                   | 23                        |
| nylon  | 26                          | 40                           | 47                   | 16                  | 26                        |
| polyester  | 106                         | 30                           | 47                   | 10                  | 15                        |
| viscose  | 65                          | 7                            | 21                   | 2                   | 16                        |
| high modulus<br>fibres (e.g.<br>UHMWPE,<br>PPTA) | 2000–35,000                 | <sup>a</sup>                 | 100–450              | <sup>a</sup>        | 0.5–5                     |

<sup>a</sup> No marked yield point.

The human body can work as an energy source for thermoelectric generators. Vladimir Leonov [55] calculated that a bulk thermoelectric generator sown on a human body's clothing for 10 hours a day, can produce energy equivalent of a similar size alkaline battery within 9 months. The generated power depends on the materials used in the TEG, the ambient temperature and the activities of the body. A thermoelectric generator with right materials can generate power in the 5-0.5 mW in ambient temperatures. This experiment was done with the state-of-the-art materials in bulk format, making it cost about ten times that of alkaline batteries.

The currently state of the art low temperature TE materials such as  $\text{Bi}_2\text{Te}_3$  and  $\text{Sb}_2\text{Te}_3$  are not very suitable for textile use. Not only is telluride, the main component of both materials, a rare earth metal that is hard to come by, it is also toxic to a human. In addition, both state-of-the-art materials are very rigid and, in that way, not a good solution for flexible textile solutions. [56]

As textile is usually relatively thin and the temperature differences are small there is an issue as the temperature on the textile equalizes quickly. This can be adjusted when considering the direction where the thermoelectric generators are placed. Lee et, al [57] produced a woven textile of specialized yarn where the temperature gradient was through the thickness of the fabric, as observed in Figure 11a. This produced a power output of

8,56 Wm<sup>-2</sup> with a temperature difference of 200 ° C. Whereas, in plane directed thermoelectric generators can be made to have a larger temperature difference with the help of insulation, as can be observed in Figure 11b. There a thermoelectric voltage of 23 mV could be obtained in room temperature with a one-legged TEG. [6]

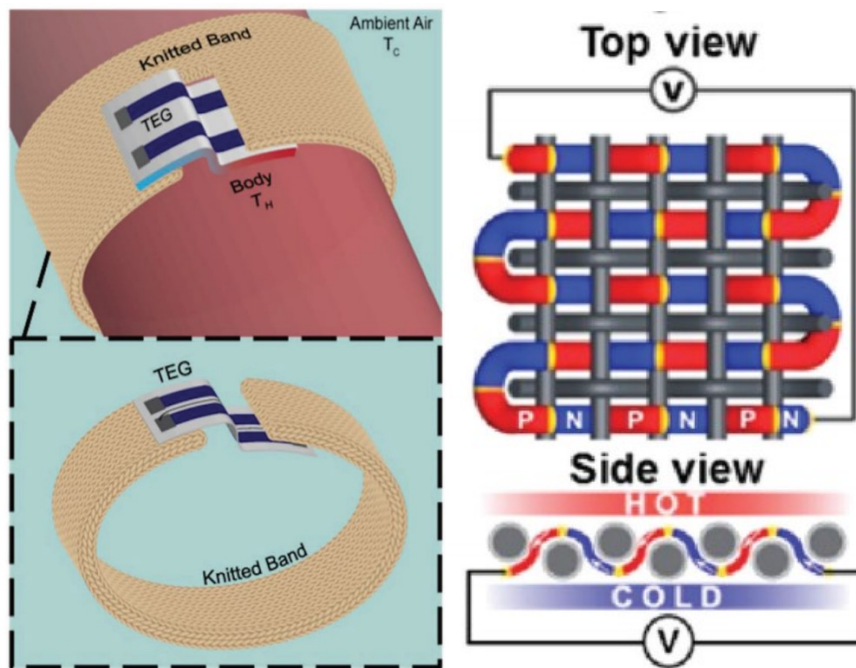


Figure 11. Thermoelectric textiles a) with a heat difference in the thickness direction (Lee, Aliev et al. 2016), b) with heat difference in the in-plane direction [6].

A prerequisite for a functional TE textile is its ability to withstand wear and tear as well as moisture and washing. In a study to test these properties for doped ZnO coated textiles they could concluded that, while withstanding a good amount of wear through folding, the coatings effects were lost after washing with water [58]. The wash resistance of a substrate and its coatings can be improved with modern functionalization such as using acid dyes and or conjugated polyelectrolytes on natural textiles, that protect the coatings from being washed away. [59]

ALD offers a highly controllable deposition technique for textile substrates. The deposition techniques and reactions are different depending on the deposited material, temperature

and the substrate used. In detailed studies of ALD on textiles it was found that inorganic fibres swelled in the higher temperatures and caused a roughened surface texture on the textile, only when the deposition could go on was there uniform growth. Figure 12 shows the different effect of deposition on inorganic fibres. [4] The high surface areas of fabrics can require longer pulse and purge times for the precursors to fully disperse in the fibre network. [22]

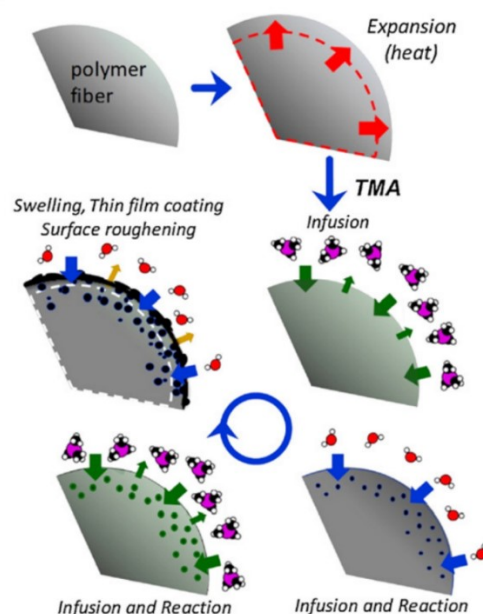


Figure 12. Effect of trimethyl aluminium (TMA) ALD on inorganic fibres. [4]

Jur et, al [60] studied ALD in 115 ° C of ZnO on a cotton substrate and found many interesting observations. The ZnO on the textile resulted in a conformal layer that imitated the original fibre structure. The more layers that were deposited the stiffer the resulting textile became. The conductivity of the ZnO was significantly lower than that of the bulk material, most likely due to cracking in thicker coatings with mechanical stress applied. The fibre structure made analysis of the formed layers also much more difficult.

The type of fabric can impact the ALD efficiency, this especially clear with area selective ALD. A study showed that nonwoven textile is more efficient at limiting lateral growth, as the woven fibres seems to lead the reactants beyond the masked areas. This can be observed in Figure 13, where different patterned textiles are deposited with ZnO using



ALD in a temperature of 155 ° C. The pattern has clearly impregnated more than the exposed area, especially with the woven material. The masks are made of aluminium and held in place with screws. [33]

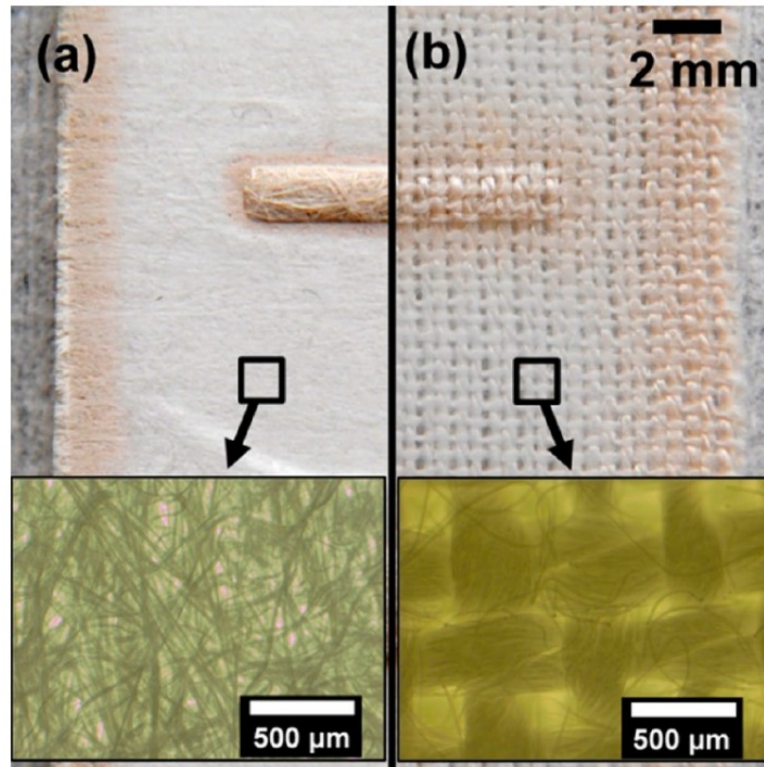


Figure 13. Area Selective ALD of ZnO using masks on a) nonwoven substrate b) woven substrate. [60]

Impregnating textile with PEDOT:PSS is a simpler process where any liquid deposition technique can be utilized. The resulting conductivity is harder to predict when it comes to textiles. Factors that affect these measurements include the weave of the textile, porosity, thickness and hydrophilicity. [44]

## EXPERIMENTAL SECTION

### 6 GOALS FOR THESE EXPERIMENTS

---

The goal of this thesis is to design a two-legged thermoelectric generator that would be suitable on a textile substrate. In this design the heat gradient is to be in the in-plane direction similar to the one-legged design proposed in Allison et al.'s report[6]. This would enable to have a greater heat difference between the different poles of the device but might cause higher resistance in the material as the conduction distance is longer.

As the goal is to fabricate this design on textile, which could be used on human skin, both chosen materials must then be nontoxic and flexible with the textile. For this reason, thermoelectric materials Zinc Oxide and PEDOT:PSS are chosen, they filled the requirements as well as having relatively easy deposition methods available. Unfortunately, there is not enough time to optimize the materials for this thesis, which could have improved the thermoelectric properties.

To understand the effect of the design on different substrates the same design is fabricated on Silicon Oxide wafers. As a substrate the wafers are more researched and understood than textile, but it has issues of being more fragile, hydrophobic and the deposited materials do not penetrate the substrate, like it does for the textile substrate. The ZnO depositions do not cause as much of an issue, since there is no need for area selective ALD with this substrate and the deposited thickness can be more accurately estimated.

To enable the proposed design on textile, area selective deposition methods are necessary to keep the different thermoelectric materials electrically isolated from each other. Depositing the ZnO selectively with ALD is an issue. ALD is known for its even and penetrating depositions, so to limit deposition areas on a woven textile substrate without using additional chemicals is a challenge.

## 7 SYNTHESIS AND CHARACTERISATION

---

This chapter presents the experiments made for this thesis and their analysis methods. It will provide the materials and methods in detail as well as motivate the reasons for these decisions. The chapter is divided in two distinct parts: Making the samples and analysis techniques.

### 7.1 MAKING THE SAMPLES

To be able to start making these samples a substrate type had to be chosen. This substrate had to be able to tolerate temperatures, up to at least 100 °C. The substrate needed to have enough of a thickness and tight enough weave so that theoretical charges could travel through. Because the plan was that the thermoelectric material impregnates the substrate material, the substrate could also not be too dense or impenetrable. To be able to reliably deposit using ALD the surface of the substrate material also needs to have active hydroxyl groups. All these factors limited the choice to natural materials, as they tolerate higher temperatures and most have active hydroxyl groups on the surface.

For this thesis three alternatives were tested. Thick 100% cotton (MATIAS, furniture fabric), thin 100% cotton (sheet fabric, 150) and typically thick 100% linen (IKEA). After some testing with spraying PEDOT:PSS to test the absorbance of the fabric and limiting spreading, the thick cotton was chosen to be the main fabric substrate. To have comparable results oxidized silicon wafers (520  $\mu\text{m}$  of  $\text{SiO}_2$ , Okmetic) were chosen to be compared with the cotton substrates. Oxidized silicon is a well-known substrate type that needed the oxide layer to be electrically insulating like the textile substrate [5]. Figure 14 shows the different fabric substrates before deposition.



*Figure 14. Fabric substrates, underneath linen, middle is thin cotton and above the chosen thick cotton.*

All images of the fabric substrates in the results have been digitally altered with GNU image manipulation program, to ensure that the deposited material would be clearly distinguishable. The images have been modified for their white balance, with an automated white balance function in the program, to make the contrast between white and deposited material higher.

#### 7.1.1 Structure concept

Designing the fabric thermoelectric generator there were important factors to be taken into consideration. First, the type of textile chosen as the substrate meant that the temperature difference would have to be in plane with the fabric. This meant that the TE material strips would need to be long enough that temperature gradient would not equalize between the different ends, at least not too quickly. They would also need to be wide enough to be properly conductive.

To test the previous factors as well as the amount of spreading over the selected areas when using ALD, a testing aluminium mask was created. This mask had differently wide gaps and they were distributed in various distances from each other so the conductivity

within could be measured as well as if the material was conductive in between the intended strips. One major limiting factor when designing was the size of the ALD reaction chamber that measured in about ~12 cm in diameter. The testing mask A was made of 2 mm thick aluminium and was produced according to the Figure 15.

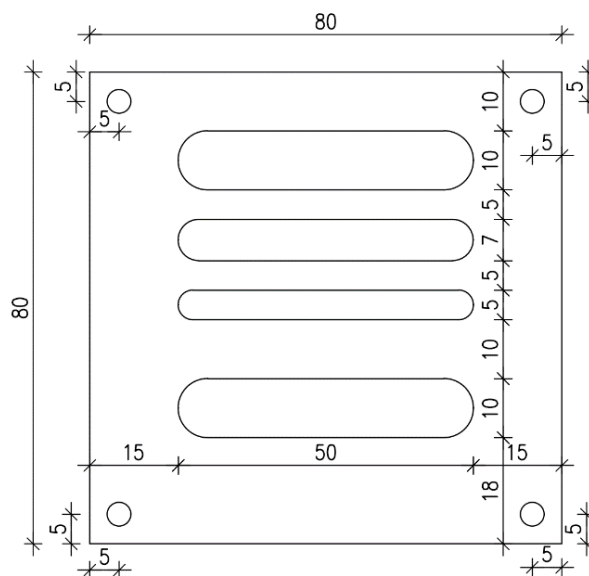


Figure 15. Aluminium mask model for testing a design concept, all measurements in millimetres.

From the designs, aluminium masks were made by a local workshop. There were two copies of all the mask designs and two same size plates without any pattern, only the four screw holes. The idea was to test the best way to get area selective ALD on the fabric substrate with two mask alternatives. One with a pattern on the top and a closed plate beneath, like the Figure 8 in Section 3.2 . Second one with the same pattern repeating on the top and the bottom, with the hypothesis that the precursors could flow through the substrate without having time to deposit between the masks. The concept of the second approach is illustrated in Figure 16. All screws were tightened with fingers without using extra tools.

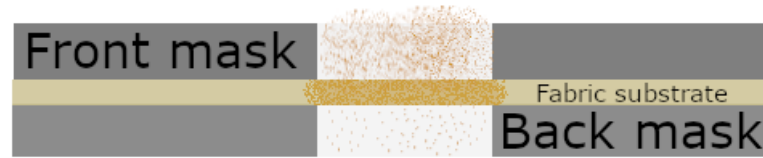


Figure 16. Open mask concept where the same pattern is repeated on both sides of the mask.

Figure 17 shows all the mask designs with the corresponding letters that they will be referred to in this thesis, all masks can be used as open or closed options, indicating the possible ALD flow options.

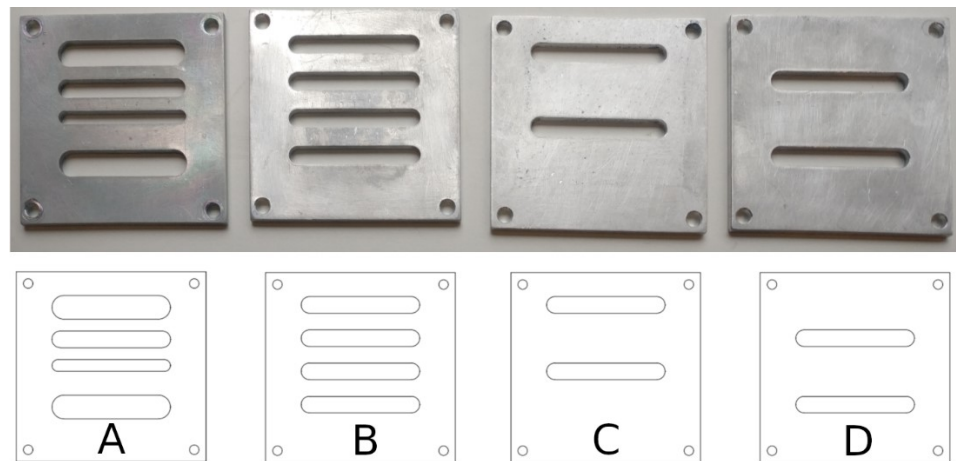
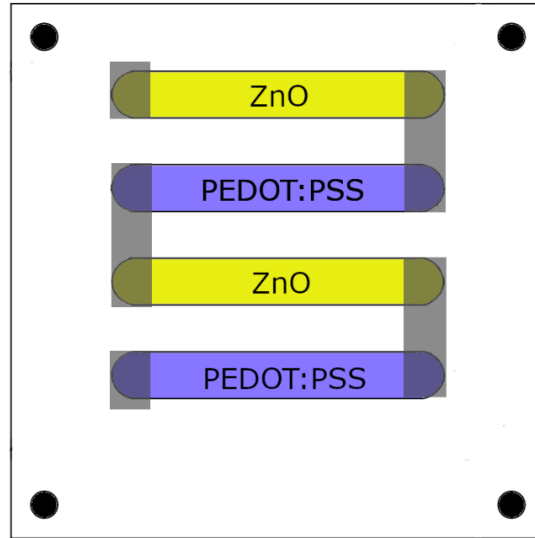


Figure 17. The different masks used in this work denoted by letters A, B, C, D

Based on some ALD testing and measurements that even a 5 mm wide strip could be conducting throughout the eventual design, the mask ended up having 2 modules as a third would not fit. The chosen parameters of the proposed design were 7 mm wide stripes with 7 mm distance between the strips, other dimensions were the same as in the test mask A, see Figure 15. The different legs and modules were connected in series with silver paste. The proposed design for a in plane thermoelectric generator for a fabric substrate is shown in Figure 18.



*Figure 18. Proposed thermoelectric design on fabric.*

The aim was to find a way to impregnate the fabric with both TE materials so that the fabric would be equally conductive on both sides of the material. This would ensure that the materials would be thick enough and that temperature gradient through the fabric would not affect the results. To ensure the deposition has impregnated the fabric the conductivity of both sides of the fabric was measured after deposition. All samples were tested for their conductivity with a digital multimeter (FLUKE, 116 true RMS multimeter), for electrical resistance ( $\Omega$ ) on both sides. The measurements were taken from the ends of the strip to make sure that the entire strip was conductive. It is important to check that the deposited material has stayed within the mask limits, to test this the conductivity was measured from line to line, as illustrated in Figure 19. The denotations of letters on the illustration shows which strip is tested and when testing for conductivity between the strips.

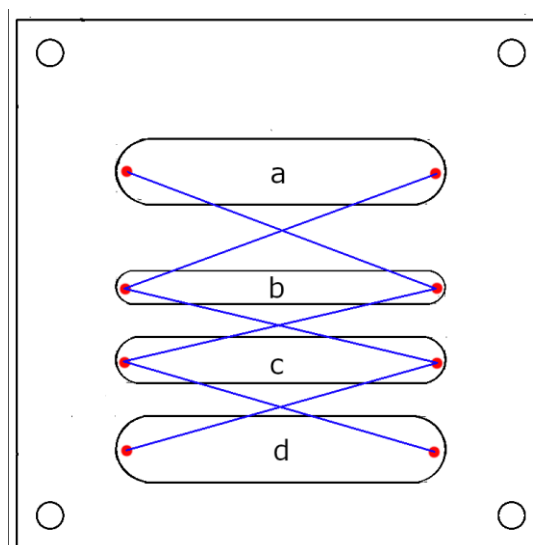


*Figure 19. Measurement points on the fabric, the red dots represent measurements within the strip and blue lines between the strips.*

For the  $\text{SiO}_2$  substrates a combination of chromium and copper was used to connect the materials in a series. Chromium and copper layers were deposited using thermal evaporation with an aluminium patterned shadow mask. Chromium was added beneath the copper layer to increase the sustainability of the copper when attaching metal masks with tape.

### 7.1.2 Area Selective Spraying

Area Selective Spraying was done using an Air-Brush (Badger, model 150) connected to a nitrogen tank. Several different ways to selectively choose deposited areas were tested for different substrates to get the best results. For the fabric substrates tape and metal masks worked to hinder unwanted depositions, so to the eventual design mask D was chosen to ensure correct placement of the substrate.

The different fabric types were tested with PEDOT: PSS (Clevios , PH 1000) spraying for analysis of impregnation, conductivity and how much it would spread. PEDOT:PSS was tested with two different approaches, letting the liquid dry or depositing all the layers without drying. The three different fabrics were covered with a big piece of tape on a piece of thick paper. The test deposited 10 layers of material on three different fabrics, in one



set a layer was left to dry for atleast 30 min before the next layer was applied and on the other set a layer was sprayed on the other without letting the previous layer dry. The dry sample set was done by cutting 10 holes in to the plastic covering the different fabrics, the holes were about 1 cm<sup>2</sup> in size and 1 cm apart. For the drying fabrics a layer was deposited and let dry, the dry square was then covered with tape before continuing the process. The process was repeated until the last box had 10 layers of PEDOT:PSS on the different fabrics. For the non-drying sample set only one box was cut out at a time and the layers were sprayed on with a approximately 5 second interval, then covered before the next layer was cut out.

When spraying the silicon oxide wafers with PEDOT:PSS another mask type was used than the ones designed for textiles. This was as there was no need for screw holes, there was more space to add an additional two legs to this substrate. The new mask had 6 stripes that were 5 cm wide and 7 mm in height. The distance between the stripes was another 7mm. Only half of the stripes were deposited with PEDOT:PSS so the remaining stripes needed to be protected. The protection was done using tape, this was to hinder the deposited material from going on to the ZnO surface as well as to keep the mask properly attached to the wafer. Figure 20 shows this other mask as well as the way it was taped on the wafer before spraying.

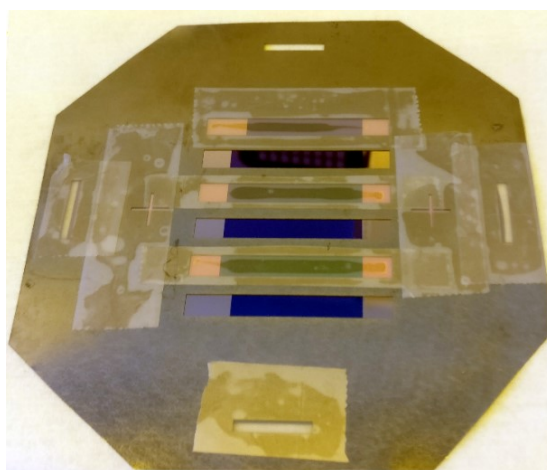


*Figure 20. Thinner aluminium mask that is taped on to a SiO<sub>2</sub> wafer.*

For the metal substrates there were some issues with the hydrophobicity of the silicon oxide when spraying. There were many test depositions of PEDOT:PSS on silicon oxide before a working technique was found. Eventually, the metal substrates were sprayed directly to the normal of the substrate, so that the liquid pressure would not force material underneath the mask. All deposited layers were thin to discourage big droplets from forming. That is why several layers (about 10) were required for a uniform layer.

All spraying was done at an approximate distance 10-20 cm from the substrate. The substrates were leaned against a wall during spraying but then immediately dropped down to a horizontal position to dry. The substrates needed to be in a vertical position due to the spraying device, had to be in a relatively horizontal position for successful spraying. To disable access beneath mask when spraying the spray had to be distributed in the normal to the plane, but also to discourage any of the liquid to trickle down beneath the mask after the spraying. This was especially important with the SiO and plastic substrates due to their hydrophobicity this is why for these substrates the stripes were kept vertical during deposition. This was done to have as little area as possible where gravity could assist the spreading. The exact thickness of the PEDOT:PSS film could not be determined on any of the substrates due to the uneven and unpredictable deposition method. For the resulting deposition, thin layers were piled on to create an even layer that was tested to be conductive.

### 7.1.3 Area Selective ALD

All ALD in this thesis was made using the Picosun R-100 ALD-reactor that is a top flow-type reactor. The samples were deposited in a 11hPA vacuum pressure and in a temperature of 80 °C. Zinc Oxide was deposited using diethyl zinc (DEZ) ( $\text{Zn} \geq 52,0 \text{ m-\%}$ , Aldrich) and de-ionized water ( $\text{H}_2\text{O}$ ) as precursors according to the Formula 2 on page 21. Nitrogen was used as purge gas in all depositions. All the fabric samples were placed between the metal plates with four hand tightened screws on a set of four copper screwable legs to keep the

sample in place, as the normal platform could not be used with the metal masks. The placement and arrangement of the masked fabric substrates can be seen in Figure 21.

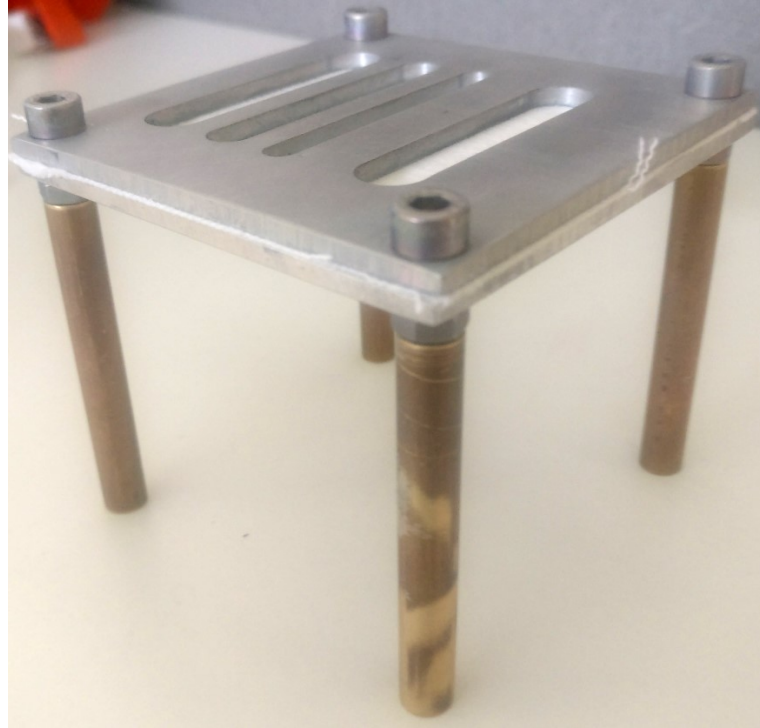


*Figure 21. Area selective ALD platform with mask A, for textile substrates.*

The experiment is set up to learn from previous sample sets to save some time. Therefore, not all sample sets include all the different variations as previous sets have. There were 4 different sample sets with Area Selective ALD on fabric. All the different sample sets, and the defining deposition settings can be observed in Table 2.

*Table 2. Area selective ALD samples and their determining factors.*

|       | Sample | Cycle | Valve<br>(s) | Backmask | Pulse (s)<br>(DEZ/H <sub>2</sub> O) | Purge<br>(s) | Mask | Deposition<br>rounds |
|-------|--------|-------|--------------|----------|-------------------------------------|--------------|------|----------------------|
| Set 1 | 1      | 600   | 10           | Open     | 0,2/0,3                             | 20           | A    | 1                    |
|       | 2      | 600   | 10           | Closed   | 0,2/0,3                             | 20           | A    | 1                    |
|       | 3      | 600   | -            | Open     | 0,2/0,3                             | 10           | A    | 1                    |
|       | 4      | 600   | -            | Closed   | 0,2/0,3                             | 10           | A    | 1                    |

|       |   |      |   |        |         |    |   |   |
|-------|---|------|---|--------|---------|----|---|---|
| Set 2 | 4 | 600  | - | Closed | 0,2/0,3 | 10 | A | 1 |
|       | 6 | 1200 | - | Closed | 0,2/0,3 | 10 | A | 1 |
|       | 7 | 1800 | - | Closed | 0,2/0,3 | 10 | A | 1 |

|       |   |      |   |        |     |    |   |   |
|-------|---|------|---|--------|-----|----|---|---|
| Set 3 | 8 | 600  | - | Closed | 1/1 | 15 | A | 1 |
|       | 9 | 1200 | - | Closed | 1/1 | 15 | A | 1 |

|       |    |      |   |        |     |    |   |   |
|-------|----|------|---|--------|-----|----|---|---|
| Set 4 | 10 | 1200 | - | Closed | 1/1 | 15 | A | 2 |
|       | 11 | 1200 | - | Closed | 1/1 | 15 | C | 2 |

The first set of samples, Set 1, was set up to test the effect of the back mask and the effect of a secondary valve to increase the reaction time in the chamber. All the samples in set 1 were slightly smaller than the mask to avoid making holes in the fabric. Consequently, determining the exact position of deposited material was hard and the tightened masks bended over the fabric. Later samples are the same size as the mask with holes holding the sample in place, which ensured that clearer measurements for the size of deposition could be determined.

The secondary valve used to fabricate the first set of samples is indicated by Valve in the table. This valve is located just after the reaction chamber and enables precursor material to be held in a reaction chamber for a longer period, which is usually needed for substrates with high surface area. A longer pulse time requires more material to travel through as a secondary valve allows a precursor to stay longer in the reaction chamber. In this experiment the precursor gas was left in the reaction chamber for 10 after the pulse. Using the valve also increases the pressure within the chamber as purge gas is constantly pumped in but not let out.

The second set of samples, Set 2, tested the effect of deposition thickness for successful area selective ALD. To determine if the area selectiveness was decent the conduciveness of the samples was measured through the deposited lines on both sides as well as between the lines. If the areas between the lines were conductive the deposition had not been

thoroughly area selective. This could also be measured visually as the ZnO surface coloured the textile to a pale yellow. Three different thicknesses were tested for this set.

The third set of samples, Set 3, had a longer pulse and purge time to let the material reaction develop. More material was pumped through the chamber to enable a more thorough deposition reaction, as a response also the purge time has to be extended so all material could be removed before the next step.

For a thorough impregnation of ZnO in the fabric a two-sided deposition technique was tested as the fourth set. The samples were deposited with the same conditions twice, once on each side of the fabric. This approach ensured that a sufficient amount of ZnO was deposited on both sides of the fabric as well as impregnated into the network.

In addition to the textile samples, the comparison samples were also made using ALD according to Table 3. There was no mask used during ALD, as the selective process was made using UV lithography and etching. To remove the extra ZnO film the chosen areas of the substrate were patterned to the surface using photoresist (AZ 1518) and UV light. Then the unwanted ZnO was etched away with a mixture of H<sub>3</sub>PO<sub>4</sub>, acetic acid and water in a ratio of 1:1:50. Acetone was then used to remove the photoresist from the surface, leaving only clean lines of ZnO.

*Table 3 ALD settings for Silicon Oxide substrates.*

|                  | Sample number | Cycles | Pulse (s)<br>(DEZ/H <sub>2</sub> O) | Purge (s) | Temp (°C) |
|------------------|---------------|--------|-------------------------------------|-----------|-----------|
| SiO <sub>2</sub> | 12            | 600    | 0,2/0,3                             | 10        | 80        |
|                  | 13            | 3200   | 0,2/0,3                             | 10        | 80        |

After selective deposition also sample 11 and the comparison samples were selectively sprayed with PEDOT:PSS from both sides. Eventually we had samples with both TE materials on the surfaces. Samples 11-13 were then tested for their thermoelectric functionality.

## 7.2 THERMOELECTRIC PERFORMANCE

The thermoelectric performance of the finished samples was evaluated using a temperature difference and measuring the induced voltage. These tests were performed on the two different SiO<sub>2</sub> samples, samples 12 and 13, as well as the one finished textile sample, sample 11. All the samples had strips of both ALD deposited ZnO and PEDOT:PSS connected in series with either copper or silver paste. The SiO<sub>2</sub> samples were tested to make sure the materials and design could be functional, and to test the effect of ZnO layer thicknesses, as the thickness on the textile substrates is harder to define. The ZnO on the silica substrates were presumed to be around 100 nm thick on sample 12 and 500 nm on sample 13.

The samples were tested by heating one side of the sample on a temperature-controlled hotplate (UniTemp GmbH) and the other side of the sample on the not heated part of the hotplate, the setting is displayed in Figure 22. The other side of the sample was kept cool with a heatsink that was cooled with a 12 V fan on top of the sample substrate. The temperature difference was closely monitored using two resistive thermometers on each side of the sample.

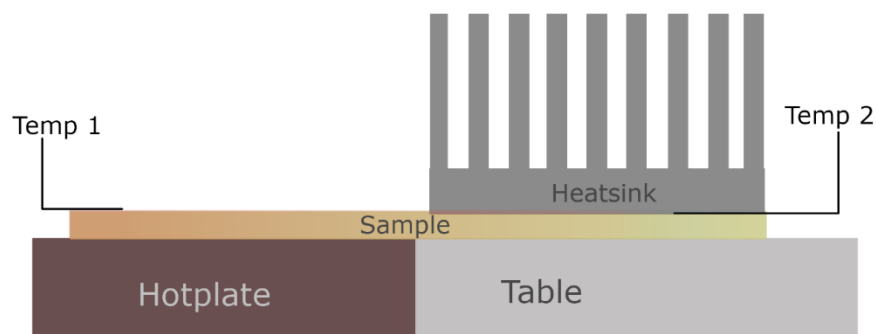


Figure 22. Measurement setup to evaluate the thermoelectric performance of the samples.

The induced voltages were measured both during heating and cooling of the hotplate, so the effect the temperature difference could be determined. The measurements are done

both with an open circuit and with a  $1.4\ \Omega$  resistance added to the circuit to determine the outcoming voltage regarding the temperature difference. As the educed power of the proposed design will be low the resistance of the TE materials needed to be as low as possible for the power to pass through. The measurement setup was controlled using a standard LABVIEW program connected to a multimeter.

## 8 RESULTS

---

This chapter will present the data obtained from the experiments discussed in Chapter 7. The results are then discussed and compared with data found in previous studies.

### 8.1 SELECTIVELY DEPOSITED PEDOT:PSS

Area selective spraying started with testing different fabric types sprayed with PEDOT:PSS, the result of this spraying is shown in Figure 23. In the figure the samples to the left have been let to dry between layers of PEDOT:PSS and the samples to the right have all the layers sprayed on top of each other without drying. It can clearly be observed that drying in between the layers let kept the PEDOT better within the selected boxes, while adding layers while the previous layer still was wet, forced the PEDOT to spread underneath the masking tape.

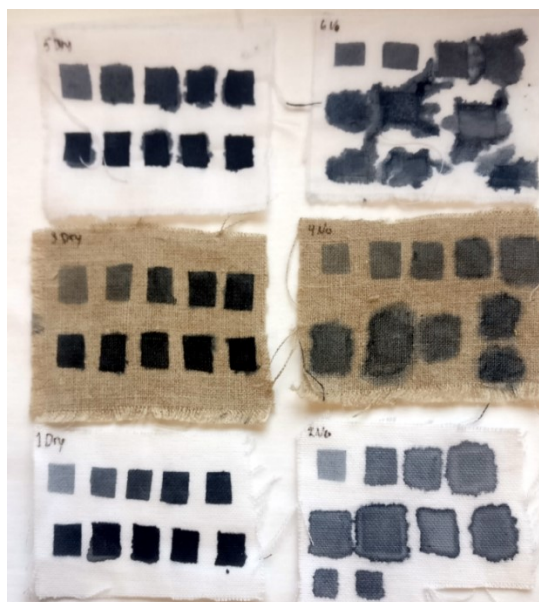


*Figure 23. PEDOT:PSS sprayed fabric samples, on the left samples have dried between layers while on the right samples have all layers added on without drying.*



In the Figure 23 the different fabrics presented are the thin cotton on the top, linen in the middle and the thick cotton on the bottom. The thin linen is hard to control and the PEDOT:PSS has spread even when the fabric has been let to dry between layers. The cleanest lines between the boxes are on the thick cotton that could absorb most of the moisture so that the liquid material could not trickle underneath the tape mask. However, while keeping the material within a selected area, for function it is also important to ensure that the material is conductive.

The resistance of the conductive PEDOT:PSS boxes can be seen in the Figures 24, 25, and 26. In Figure 24 the resistance measured from the front side of the fabric from the dried samples can be observed. The trend is logical, the more material on the fabric the lower the resistance in that material. None of the boxes with only one layer of material were conductive enough to measure. The thick cotton had the lowest resistance of all the materials, most likely due to the tick weave between the fibres. After the eighth layer the PEDOT:PSS adding more layers does not significantly reduce the electrical resistance.

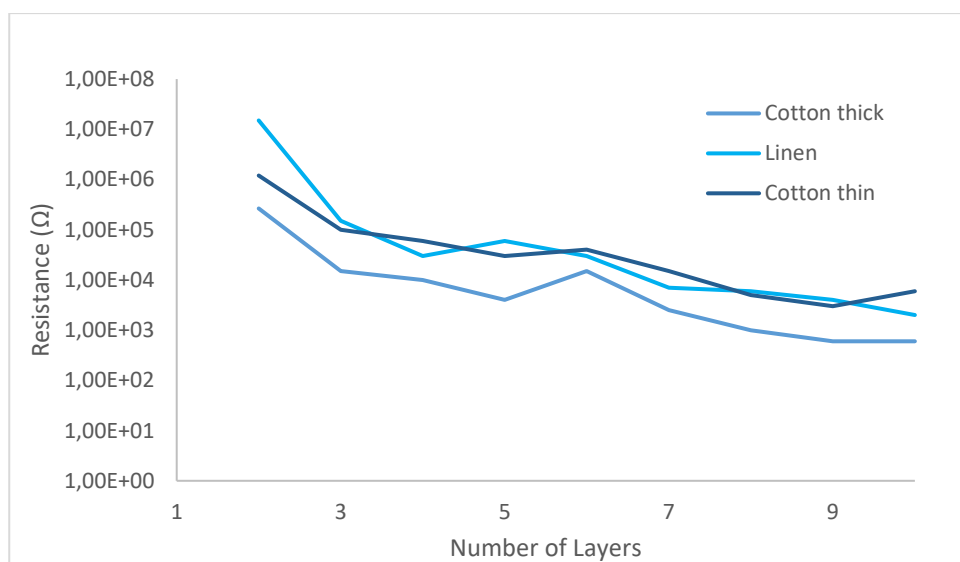


Figure 24. Electrical resistance of PEDOT:PSS measured from the sprayed surface

Similar to the drying samples the wet layered samples electrical resistance of PEDOT:PSS lowered as the thin film got thicker. Figure 25 shows that the resistance in average is

higher than in the dried samples. This is most likely due to a thinner layer of solid PEDOT:PSS material in one area when comparing to the dry version. From these results the material thick cotton was chosen to be used, this was because it was easier to spray area selectively as well as having the lowest resistance values when sprayed with PEDOT:PSS.

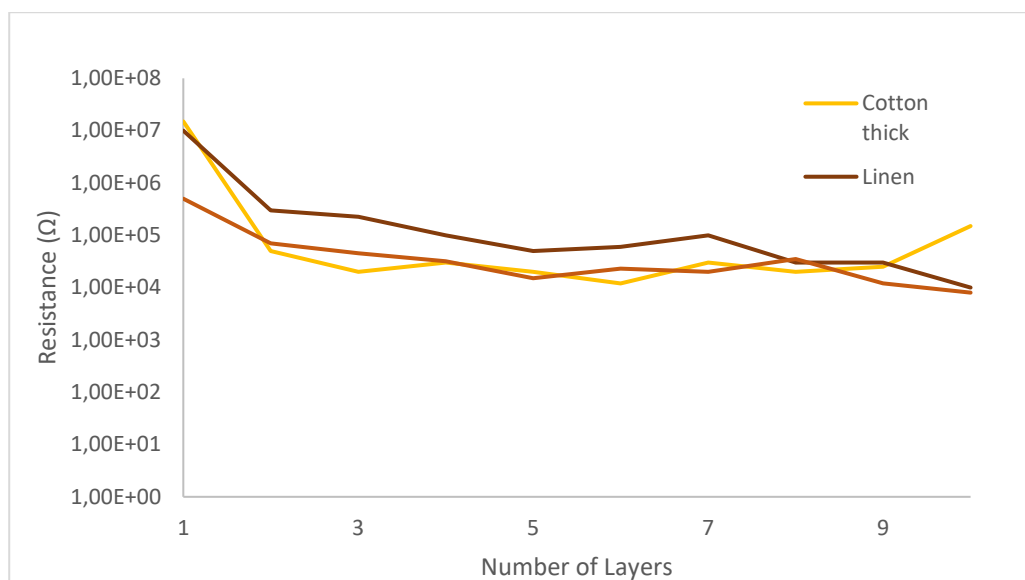


Figure 25. Electrical resistance of wet deposited samples when adding layers of PEDOT:PSS

Figure 26 shows the results of all fabric samples back sides for their electrical resistance. Little material in the thick cotton that was let to dry penetrated the fabric to be fully conductive on the other side, resulting in that data is not available in the figure. The back side of the material had in average much higher resistance than that of the front sides again as there was less material that had gone through. The resulting resistivity was much more unpredictable and harder to measure, but in general the wet samples had a lower resistance on the back of the fabric.

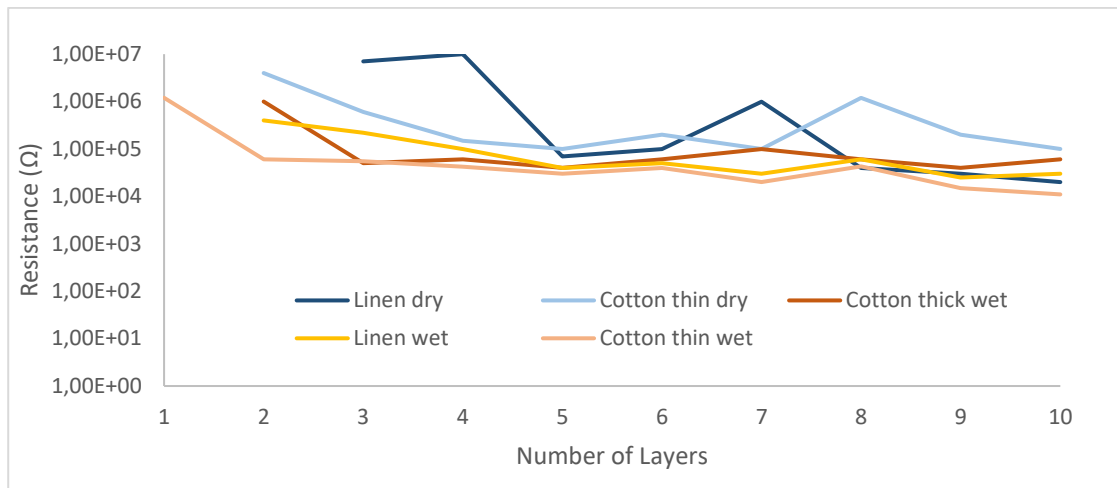
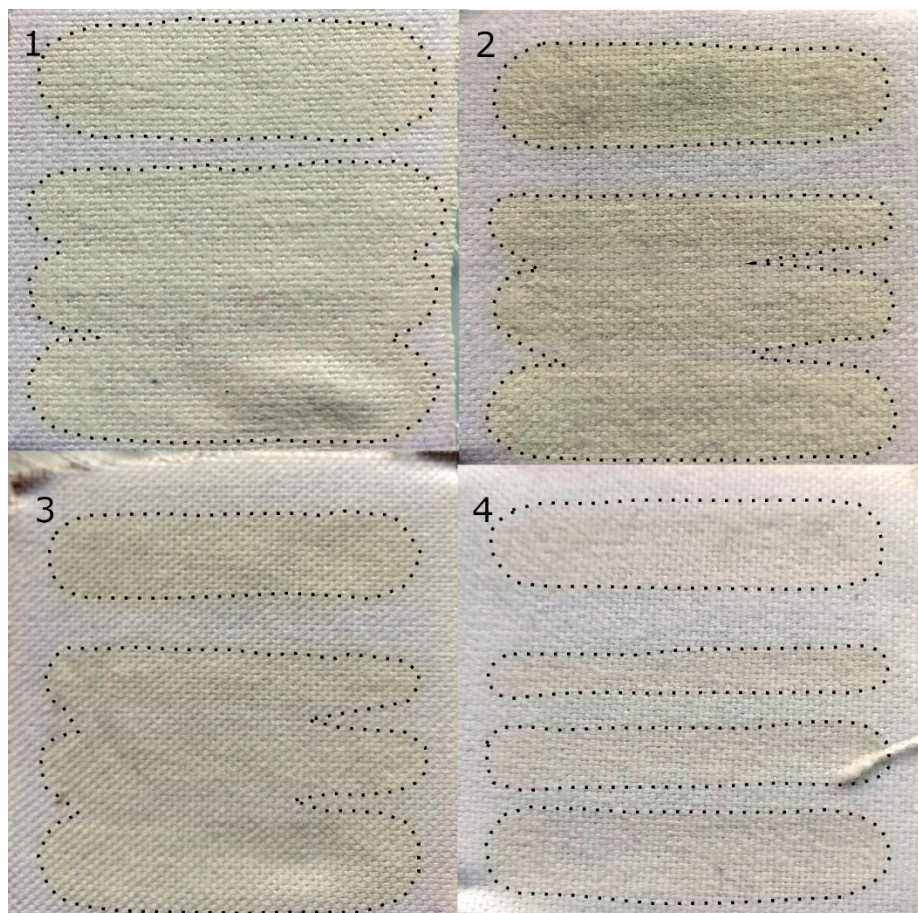


Figure 26. Electrical resistance measured from the back of the fabrics.

As the average thickness of the samples is hard to determine due to the uneven structure of textile, the resulting resistance is hard to compare with other research. In average PEDOT:PSS has an electrical resistance of 150-300 k  $\Omega$  when used as thin films, depending on the thickness and solution [61]. Therefore, the resistance measured from the sprayed side of the samples have come close to these results when considering an average distance across a 1 cm<sup>2</sup> deposited square.

## 8.2 SELECTIVELY DEPOSITED ZINC OXIDE

The first set of samples are shown in Figure 27, in numerical order. The deposited areas are shown with a yellow tone. Even as the images have been modified the resulting deposition can be hard to distinguish. What can be seen however, is that sample 4 has the clearest lines of all these samples. The only problem with the fourth sample is that it is not conductive, neither is the third. There simply is not enough conductive material on that sample to overcome the resistance of fabric.



*Figure 27. Sample set 1, with samples on the left with the open mask, and on the right the closed mask. Dotted lines mark the approximate border of ZnO spread.*

The top row samples, 1 and 2, are conductive, although with quite a high average resistance of  $\sim 9 \text{ M } \Omega$  on the front side and  $\sim 17 \text{ M } \Omega$  from the back side. The two samples were both deposited using the extra valve, letting the precursor materials react for a longer time. This clearly resulted in more thorough depositions, which can be observed from the figure as well. Both samples were also conductive through the whole bottom section of three stripes with a similar resistance of that on the stripes alone. The only separate stripe was the one above that was not conductive with the rest.

The open mask seemed to have an adverse effect on deposition precision. Both open mask samples seemed to have spread more than that of the closed ones. The ones with the closed masks had more distinct areas of exposure than the open ones where the lines between stripes are hard to distinguish at all. This result is most likely due to less pressure

in the areas where the pattern was, so the reaction could travel along the fibres underneath the mask, similar to the study with ALD on nonwoven materials where masked pattern spread more with less pressure [32]. The back closed mask forced the fabric to be compressed against the pattern so less material could pass beneath the mask. A contributing factor may also be the small sizes of the samples that were not tightened in any way to the masks allowing for more movement and flexibility. This can be observed in sample 1 where the last stripe has bulged due to the open mask a most likely some pressure that made it come out more from between the mask.

The second set tested more the effect of deposition thickness. As the set with 600 cycles was not conductive when deposited in a way that was area selective, the samples with 1200 and 1800 cycles are compared in Figure 28. A layer of the proposed mask is placed on top of the images to show where the limits of the mask would go, all image placement has been according to the screw holes in the fabric. From the figure it can be observed that the 1200 cycle version stayed significantly better within the mask compared to the 1800 cycle sample where the deposition has spread beyond the mask lines.

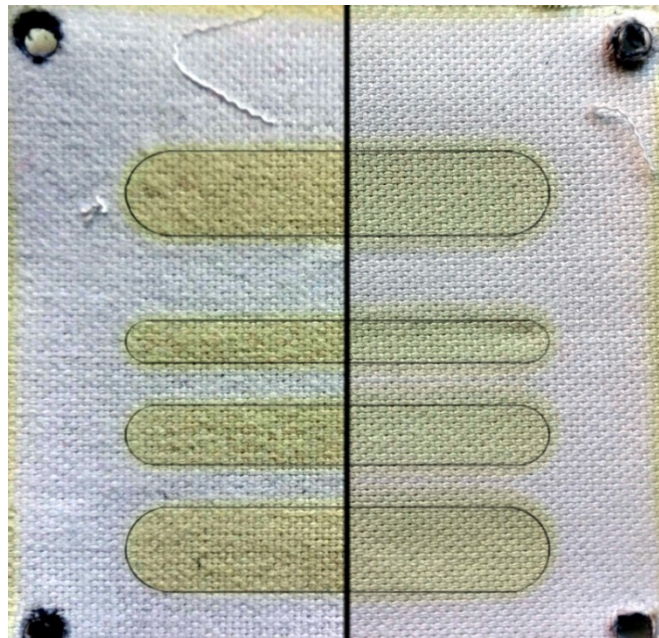


*Figure 28. ZnO deposited samples with the 1200 cycle sample to the left and 1800 cycle sample to the right.*

Of these samples only the 1800 cycle version was conductive. However, it was conductive also beyond the deposited stripes, with a resistance that could be measured from line b all the way to stripe d. The measured resistance of the 1800 cycle samples were an average of  $\sim 200\text{ k}\Omega$  from the front and  $\sim 310\text{ k}\Omega$  from the back. The resistance of the 1800 cycle sample was sufficiently better than those deposited using the valve, but there was a resistance of  $720\text{ k}\Omega$  through the stripes b to d, on both sides. 1800 cycles deposition had good conductivity, but the deposited material had simply spread too much for a feasible design.

Therefore, longer purge and pulse times were used to make sure enough material would be deposited for better conductivity without losing the area selectiveness. With a pulse time of 1 second samples for 600 and 1200 cycles were deposited. The resulting samples were very similar to those in the previous set of similar cycles, where the deposited material stayed within the selected pattern and they were not conductive. The sample with 1200 cycles did not seem far from the sought-out result as it was a little conductive on the front side. A little meaning that sometimes the multimeter gave a result with a high resistance but the result was not consistent or readable.

The sample that was deposited with 1200 cycles and a pulse time of 1 second was deposited again, this time with the other side facing upward. The resulting sample is shown in Figure 29. As the texture of the fabric is different on each side the depositions look slightly different but are of the same sample. The deposited material has distinct stripes that do not connect with each other, while there is more likely more material deposited than with the 1800 cycle sample.



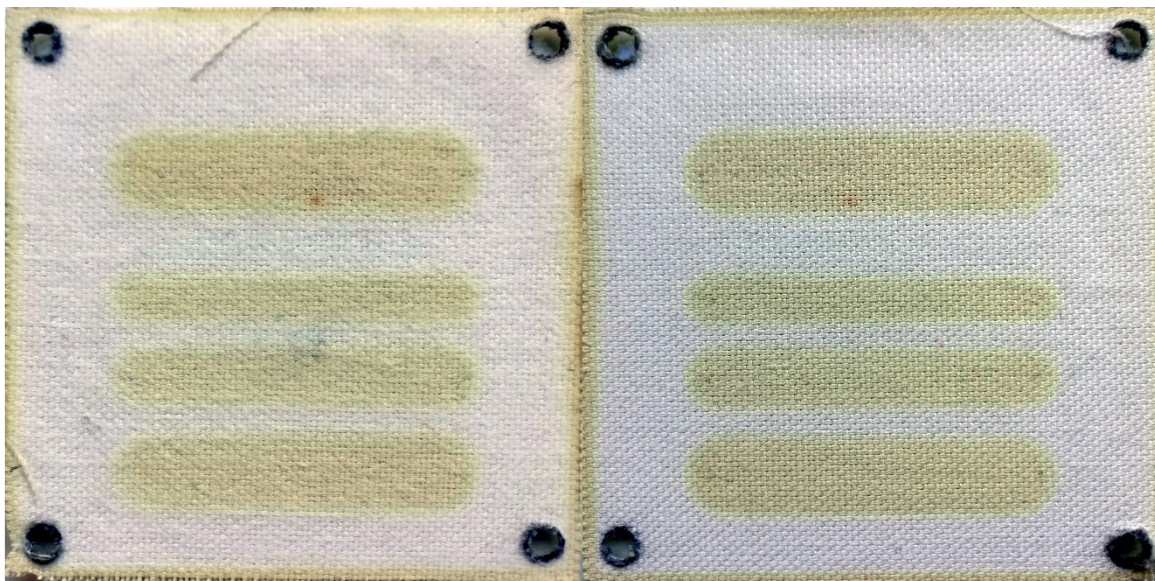


*Figure 29. Image of a twice ZnO deposited textile from both sides of the fabric.*

The electrical conductivity of the double coated sample is good, with an average resistance of  $\sim 80 \text{ k}\Omega$  on the first deposited side and an average resistance of  $\sim 50 \text{ k}\Omega$  on the other side. The lowest resistances measured in this thesis for ZnO thin films. The results were so good this was chosen to be the way to make a sample of the proposed design. The resulting sample, that was ALD coated using the same settings but with mask C and then area selectively sprayed with PEDOT:PSS similarly from both sides is shown in Figure 30.

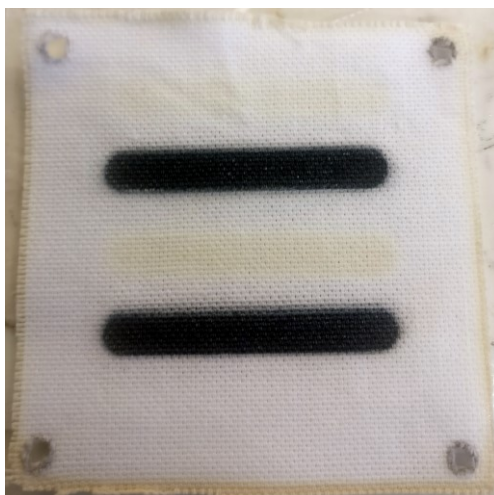


*Figure 30. Area selectively deposited two material fabric sample 11.*

Unfortunately, there is need to note that the first stripe of ZnO is lighter than the second (middle) stripe on the sample 11. This is likely due to a uneven deposition on the textile, resulting in that the resistance in the first stripe is significantly higher (3,3  $M\Omega$ ) than that of the second stripe with a resistance of only 330  $k\Omega$ . The direction of the mask in proportion to the precursor flow direction can also be a contributing factor. To determine if the deposition can be done more evenly would require making more tests with the same mask.

### 8.3 THERMOELECTRIC CHARACTERISTICS

The thermoelectrical devices are shown in Figure 31. Zinc oxide layers are shown as yellow stripes on the substrate and PEDOT:PSS as the dark blue stripes. With the different thicknesses of ZnO the depositions on the Silicon oxide wafers have a slightly different color. To measure the thermoelectric effect of these samples thin copper wires were attached with silver paste to the ends of the series. To ensure the combined resistance would not be too high, the total resistance was measured as well as the individual stripes.

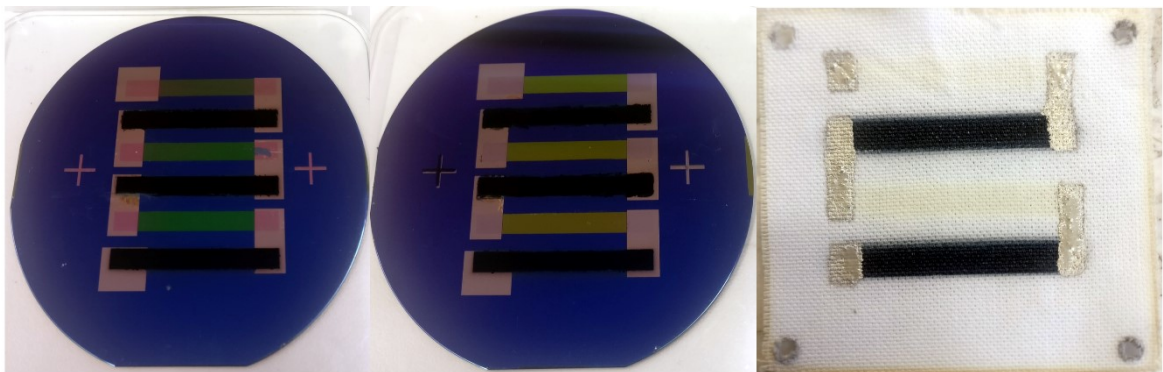


*Figure 31. Thermoelectric devices, sample 13 to the left with a ZnO thickness of 500nm, Sample 12 in the middle with a 100 nm ZnO layer and the thermoelectric textile Sample 11.*

The temperature on the hot side stayed at 10-20 °C below that of the hotplate for the Silicon samples, resulting in a maximum measured temperature difference of 70 °C. The cold side arose from a room temperature (22,5 °C ) to at its highest to 32 °C with the same



samples. Even with slow heating at 10 degrees at a time, waiting for 2 minutes up to a hotplate temperature at 110 °C a temperature difference of 50 °C could be achieved. For the textile substrate the situation was a bit different as it did not conduct heat in the same way. The maximal temperature difference between the two ends was only 21 °C with temperature rising to a 45 °C on the hot side and the cool side only to a 24 °C with a hotplate at 110 °C. The temperature difference would have most likely risen slightly with a longer measurement time, but this is the point where the temperature difference slowed down significantly when the textile sample was heated.

The resistance of each stripe as well as the total resistance of each sample are shown in Table 4. Each stripe is measured at each end, for ~5cm. The total measured distance in the SiO<sub>2</sub> device is ~30 cm and for the textile ~23cm. Unfortunately, all the thermoelectrical samples produced only a voltage that was less than 1 µV even with a temperature difference of 70 °C between the different ends of the devices. The result was unexpected but is most likely due to the high total resistance of the devices. The educed voltage could not efficiently overcome the resistance of the individual stripes in a series.

*Table 4. Resistance of the TE samples*

| Sample         | <b>13</b>  | <b>12</b>   | <b>11</b>  |
|----------------|------------|-------------|------------|
| <b>stripes</b> | (Ω)        | (Ω)         | (Ω)        |
| PEDOT          | 9k         | 15 k        | -          |
| ZnO            | 10k        | 2 M         | 3,3 M      |
| PEDOT          | 10k        | 10 k        | 8 k        |
| ZnO            | 9k         | 26 M        | 303 k      |
| PEDOT          | 8.5k       | 11 k        | 6 k        |
| ZnO            | 7k         | 2,8 M       | -          |
| <b>Total</b>   | <b>74k</b> | <b>32 M</b> | <b>33M</b> |

While it was expected that the thermoelectric textile might not work with the extremely high combined resistance, a result of some kind was expected to be gotten from the SiO<sub>2</sub> samples. The expected result was thought to be something near the results achieved by Marin et al. [5] when using a different kind of design and only with one type of material, where an electrical power output was achieved from only ZnO layers that was measured to be 0.23 µW/m<sup>2</sup>. However, this was not achieved with these samples.

One explanation could be a simple defect in the samples that is not visible and thus the thermoelectric properties could not be measured. This could be re-evaluated with making more samples with the same experimental setup and test their performance. Unfortunately, there was not enough time to do this during this thesis, especially when there have been constant issues with the ALD reactor used during this thesis.

One contributing factor of these results can be the measurement equipment that currently could not show results below 0,000001 V, which resulted in that while a small electrical power output was measured by the multimeter the recording system could not display these results accurately. With these results some comparisons between the different substrates could be analysed or interpreted for a more specific result.

## 9 CONCLUSIONS AND DISCUSSION

---

This thesis has designed and fabricated a functional two-legged thermoelectric generator on a textile substrate. The thesis has also shown that the same design can be utilized on other substrate types. This proposed design utilizes the temperature gradient along the in-plane direction of the fabric to generate power. The design uses two material types that are nontoxic and remain flexible after deposition into the substrate.

Although a miniscule amount of power output was measured from all the measured samples, the results were not as good as expected. The proposed design based on two different types of materials for an in-plane heat direction has not been tested before and will require much more research before fully understanding the functionality of the design. While the thermoelectric function would have been a great addition, the thesis nevertheless has made a significant contribution through the development of a working fabrication method of a design that could prove to be useful for other thermoelectric applications.

This study was able to successfully deposit a sufficient amount of ZnO using area selective ALD for realizing a conductive surface on both sides of the fabric. As pure ZnO is not an ideal thermoelectric material, it would be interesting to test whether the same deposition methods could be achieved when adding dopants, such as aluminium, to improve the thermoelectric performance. Because ALD is affected by so many parameters, it was not possible within the time constraints of this thesis to test more parameter combinations. Therefore, future work could also test whether thicker ZnO layers could be applied to the textile surface while still maintaining area selectiveness.

A relatively low electrical resistance for PEDOT:PSS was achieved on both SiO<sub>2</sub> and textile substrates, when selectively deposited by spraying. A surprisingly consistent electrical resistance of ~10 kΩ was measured for all sample stripes independent of the substrate, even as the process of deposition was somewhat different, and the deposited thicknesses can vary between the stripes. Surprisingly, the resistance seemed to be slightly lower on

the textile substrates than on SiO<sub>2</sub> substrates, even with the more complicated woven structure.

The methods for determining the thermoelectric performance in this work have not been ideal. After initial problems calibrating two thermometers with the existing multimeter and finding a working measurement structure, it was not possible to attain any readable results. In the future, a more sensitive measurement system, scalable even to very small voltages ( $> 1 \mu\text{V}$ ), would be needed in order to measure the thermoelectric power output of the designed fabric.

The measuring system showed that a significant temperature difference between the different sides of the substrates could be obtained in higher temperatures. For the SiO<sub>2</sub> this meant a temperature difference settled at about 70 °C when heating the hotplate to 110 °C, and a temperature difference of 21 °C on the textile substrate. This could mean that when using an insulator between the two ends, a greater temperature difference can be obtained even in room temperature applications.

When the issues realised by this thesis are overcome, a similar design concept could be utilized for thermoelectric powering of health sensors or wearable gadgets that only require small amounts of constant power to function. With additional protective coatings the system can become sustainable and durable for longer uses. While realising this potential the reality of the potential applications is still under development and requires further research.

It would be ideal to develop this proposed design with optimized materials, thicker deposited films and clearer understanding of how the deposited material attached to the fabric. Further research is needed to understand the limitations of the design and if it can be utilized for practical applications. It would be interesting test a functional design worn on a body for a longer period of time and measure the resulting power, to understand the effect it could have on the eventual applications.

## REFERENCES

---

- [1] M. Stoppa and A. Chiolerio, "Wearable electronics and smart textiles: a critical review," *sensors*, vol. 14, no. 7, pp. 11 957–11 992, 2014.
- [2] H. Song, Y. Qiu, Y. Wang, K. Cai, D. Li, Y. Deng, and J. He, "Polymer/carbonnanotube composite materials for flexible thermoelectric power generator," *Com-posites Science and Technology*, vol. 153, pp. 71–83, 2017.
- [3] G. J. Snyder and E. S. Toberer, "Complex thermoelectric materials," *Nature Materials*, vol. 7, no. 2, pp. 105–114, Feb 2008. [Online] . Available: <http://dx.doi.org/10.1038/nmat2090>
- [4] H. Brozena, C. J. Oldham, and G. N. Parsons, "Atomic layer deposition on polymer fibers and fabrics for multifunctional and electronic textiles," *Journal of Vacuum Science Technology A Vacuum, Surfaces, and Films*, vol. 34, no. 1, p. 010801, 2016.
- [5] G. Marin, T. Tynell, and M. Karppinen, "Flexible thermoelectric modules based on ald-grown zno on different substrates," *Journal of Vacuum Science Technology A Vacuum, Surfaces, and Films*, vol. 37, no. 2, p. 20906, Mar 2019. [Online] . Available: <http://dx.doi.org/10.1116/1.5079614>
- [6] L. K. Allison and T. L. Andrew, "A wearable all-fabric thermoelectric generator," *Advanced Materials Technologies*, p. 1800615, Jan 22, 2019.
- [7] J. Vineis, A. Shakouri, A. Majumdar, and M. G. Kanatzidis, "Nanostructured thermoelectrics: Big efficiency gains from small features," *Advanced materials (Deerfield Beach, Fla.)*, vol. 22, no. 36, pp. 3970–3980, Sep 22, 2010. [Online] . Available: <https://www.ncbi.nlm.nih.gov/pubmed/20661949>
- [8] J. Loureiro, N. Neves, R. Barros, T. Mateus, R. Santos, S. Filonovich, S. Reparaz, C. M. Sotomayor-Torres, F. Wyczisk, and L. Divay, "Transparent aluminium zinc oxide thin films with enhanced thermoelectric properties," *Journal of Materials Chemistry A*, vol. 2, no. 18, pp. 6649–6655, 2014.
- [9] J.-Y. Kim, W. Lee, Y. H. Kang, S. Y. Cho, and K.-S. Jang, "Wet-spinning and post-treatment of cnt/pedot:pss composites for use in organic fiber-based thermoelectric generators," *Carbon*, vol. 133, pp. 293–299, Jul 2018. [Online]. Available:

<https://www.sciencedirect.com/science/article/pii/S000862231830284751>

- [10] N. Wu, S. Linderöth, N. Pryds, and N. Nong, "Development and processing of p-type oxide thermoelectric materials," Jan 1, 2014. [Online] . Available: <https://www.openaire.eu/search/publication?articleId=od1202::23aedee9f31b0c40c0b60120b9eeda62>
- [11] S. Patil, R. R. Arakerimath, and P. V. Walke, "Thermoelectric materials and heat exchangers for power generation – a review," Renewable and Sustainable Energy Reviews, vol. 95, pp. 1–22, Nov 2018. [Online] . Available: <https://www.sciencedirect.com/science/article/pii/S1364032118305070>
- [12] Y. Du, J. Xu, B. Paul, and P. Eklund, "Flexible thermoelectric materials and devices," Applied Materials Today, vol. 12, pp. 366–388, Sep 2018. [Online] . Available: <https://www.sciencedirect.com/science/article/pii/S2352940718302804>
- [13] C.-T. Hsu, G.-Y. Huang, H.-S. Chu, B. Yu, and D.-J. Yao, "Experiments and simulations on low-temperature waste heat harvesting system by thermoelectric power generators," Applied Energy, vol. 88, no. 4, pp. 1291–1297, 2011. [Online] . Available: <https://www.sciencedirect.com/science/article/pii/S0306261910004009>
- [14] Zhigang, H. Guang, Y. Lei, C. Lina, and Z. Jin, "Nanostructured thermoelectric materials: current research and future challenge," Progress in Natural Science: Materials International, vol. 22, no. 6, pp. 535–549, 2012. [Online] . Available: <http://lib.cqvip.com/qk/85882X/201206/690757489201206005.html>
- [15] T. M. Tritt and M. A. Subramanian, "Thermoelectric materials, phenomena, and applications: A bird's eye view," MRS Bulletin, vol. 31, no. 3, pp. 188–198, Mar 1, 2006. [Online] . Available: [http://journals.cambridge.org/abstract\\_S088376940000991X](http://journals.cambridge.org/abstract_S088376940000991X)
- [16] J. W. Fergus, "Oxide materials for high temperature thermoelectric energy conversion," pp. 525–540, 2012, iD: 271630. [Online] . Available: <http://www.sciencedirect.com.libproxy.aalto.fi/science/article/pii/S0955221911005036>
- [17] Q. Wu and J. Hu, "Waterborne polyurethane based thermoelectric composites and their application potential in wearable thermoelectric

textiles,"Composites 52Part B, vol. 107, pp. 59–66, Dec 15, 2016. [Online] .  
Available:  
<https://www.sciencedirect.com/science/article/pii/S1359836816304504>

- [18] S. M. George, "Atomic layer deposition: An overview,"Chemical Reviews,vol. 110, no. 1, pp. 111–131, Jan 1, 2010. [Online]. Available:  
<https://www.ncbi.nlm.nih.gov/pubmed/19947596>
- [19] M. Leskelä and M. Ritala, "Atomic layer deposition chemistry: recent developments and future challenges,"Angewandte Chemie International Edition, vol. 42,no. 45, pp. 5548–5554, 2003.
- [20] M. Leskelä and M. Ritala, "Atomic layer deposition (ald): from precursors to thin film structures,"pp. 138–146, 2002. [Online]. Available:  
<https://www.sciencedirect.com/science/article/pii/S0040609002001177>
- [21] M. Ritala and M. Leskelä,Atomic layer deposition, ser. Handbook of ThinFilms. Elsevier, 2002, pp. 103–159.
- [22] R. W. Johnson, A. Hultqvist, and S. F. Bent, "A brief review ofatomic layer deposition: from fundamentals to applications,"MaterialsToday, vol. 17, no. 5, pp. 236–246, Jun 2014. [Online]. Available:  
<https://www.sciencedirect.com/science/article/pii/S1369702114001436>
- [23] M. Ritala and J. Niinistö, "Industrial applications of atomic layer deposition,"ECS transactions, vol. 25, no. 8, pp. 641–652, 2009.
- [24] Holmqvist, T. Törndahl, and S. Stenström, "A model-based methodology forthe analysis and design of atomic layer deposition processes—part i: Mechanisticmodelling of continuous flow reactors,"Chemical engineering science, vol. 81,pp. 260–272, 2012.
- [25] R. L. Puurunen, "Surface chemistry of atomic layer deposition: A case studyfor the trimethylaluminum/water process,"Journal of Applied Physics, vol. 97,no. 12, p. 121301, Jun 15, 2005.
- [26] R. Matero, A. Rahtu, M. Ritala, M. Leskelä, and T. Sajavaara, "Effect of waterdose on the atomic layer deposition rate of oxide thin films,"Thin Solid Films,vol. 368, no. 1, pp. 1–7, 2000.53

- [27] Kim, H. Kang, J.-M. Kim, and H. Kim, "The properties of plasma-enhanced atomic layer deposition (ald) zno thin films and comparison with thermal ald," *Applied Surface Science*, vol. 257, no. 8, pp. 3776–3779, 2011.
- [28] J. L. V. Hemmen, S. Heil, J. H. Klootwijk, F. Roozeboom, C. J. Hodson, M. V. de Sanden, and W. Kessels, "Plasma and thermal ald of al<sub>2</sub>o<sub>3</sub> in a commercial 200 mm ald reactor," *Journal of the Electrochemical Society*, vol. 154, no. 7, p. G169, 2007.
- [29] S. M. George, B. Yoon, and A. A. Dameron, "Surface chemistry for molecular layer deposition of organic and hybrid organic-inorganic polymers," *Accounts of chemical research*, vol. 42, no. 4, pp. 498–508, Apr 21, 2009. [Online]. Available: <https://www.ncbi.nlm.nih.gov/pubmed/19249861>
- [30] P. Sundberg and M. Karppinen, "Organic-inorganic thin films from ticl<sub>4</sub> and 4-aminophenol precursors: A model case of ald/mld hybrid-material growth?" *European Journal of Inorganic Chemistry*, vol. 2014, no. 6, pp. 968–974, Feb 2014.
- [31] R. Chen, H. Kim, S. Bent, D. Porter, and P. McIntyre, "Achieving area-selective atomic layer deposition on patterned substrates by selective surface modification," *Applied Physics Letters*, vol. 86, no. 19, p. 3, May 4, 2005. [Online]. Available: <http://dx.doi.org/10.1063/1.1922076>
- [32] Sinha, D. W. Hess, and C. L. Henderson, "Area selective atomic layer deposition of titanium dioxide: Effect of precursor chemistry," *Journal of Vacuum Science Technology B: Microelectronics and Nanometer Structures*, vol. 24, no. 6, pp. 2523–2532, Nov 2006. [Online]. Available: <http://dx.doi.org/10.1116/1.2359728>
- [33] W. J. S. III, C. J. Oldham, and G. N. Parsons, "Atomic layer deposition of metaloxide patterns on nonwoven fiber mats using localized physical compression," *ACS applied materials & interfaces*, vol. 6, no. 12, pp. 9280–9289, 2014.
- [34] N. Parsons, "Functional model for analysis of ald nucleation and quantification of area-selective deposition," *Journal of Vacuum Science Technology A Vacuum, Surfaces, and Films*, vol. 37, no. 2, p. 20911, Mar 2019. [Online]. Available: <http://dx.doi.org/10.1116/1.505428554>



- [35] B. Zhang, "Promising thermoelectric properties of commercial PEDOT:PSS materials and their Bi<sub>2</sub>Te<sub>3</sub> powder composites," *ACS Applied Materials and Interfaces*, vol. 2, no. 11, p. 3170, 2010.
- [36] Nardes, M. M. Kemerink, R. R. Janssen, J. J. Bastiaansen, N. Kiggen, B. B. Langeveld-Voss, A. van Breemen, and de Kok MM, "Microscopic understanding of the anisotropic conductivity of PEDOT:PSS thin films," *Advanced Materials*, vol. 19, no. 9, pp. 1196–1200, 2007. [Online]. Available: <https://www.narcis.nl/publication/RecordID/oai:library.tue.nl:640907>
- [37] M. Nardes, M. Kemerink, M. M. de Kok, E. Vinken, K. Maturova, and R. A. J. Janssen, "Conductivity, work function, and environmental stability of PEDOT:PSS thin films treated with sorbitol," *Organic Electronics*, vol. 9, no. 5, pp. 727–734, 2008. [Online]. Available: <https://www.sciencedirect.com/science/article/pii/S1566119908000906>
- [38] J. Luo, D. Billep, T. Waechtler, T. Otto, M. Toader, O. Gordan, E. Sheremet, J. Martin, M. Hietschold, and D. R. Zahn, "Enhancement of the thermoelectric properties of PEDOT:PSS thin films by post-treatment," *Journal of Materials Chemistry A*, vol. 1, no. 26, pp. 7576–7583, 2013.
- [39] O. Bubnova, Z. U. Khan, A. Malti, S. Braun, M. Fahlman, M. Berggren, and X. Crispin, "Optimization of the thermoelectric figure of merit in the conducting polymer poly(3,4-ethylenedioxythiophene)," *Nature Materials*, vol. 10, no. 6, pp. 429–433, Jun 1, 2011. [Online]. Available: <https://www.ncbi.nlm.nih.gov/pubmed/21532583>
- [40] Y. Chonan, N. Sato, T. Komiyama, K. Kotani, and H. Yamaguchi, "Enhancement of thermoelectric properties of PEDOT:PSS films by applying an alternating electric field during preparation," *Journal of Electronic Materials*, pp. 1–5, Mar 1, 2019. [Online]. Available: <https://search.proquest.com/docview/2195743661>
- [41] Q. Wei, M. Mukaida, K. Kirihaara, Y. Naitoh, and T. Ishida, "Recent progress on PEDOT-based thermoelectric materials," pp. 732–750, Feb 1, 2015. [Online]. Available: <https://www.ncbi.nlm.nih.gov/pubmed/28787968>
- [42] L. V. Kayser and D. J. Lipomi, "Stretchable conductive polymers and composites based on PEDOT and PEDOT:PSS," *Advanced Materials*, 55 vol. 31, no. 10, p. n/a, Mar 8, 2019. [Online]. Available: <https://onlinelibrary.wiley.com/doi/abs/10.1002/adma.201806133>

- [43] U. Lang, E. Müller, N. Naujoks, and J. Dual, "Microscopical investigation of PEDOT:PSS thin films," *Advanced Functional Materials*, vol. 19, no. 8, pp. 1215–1220, Apr 23, 2009.
- [44] M. Vosgueritchian, D. J. Lipomi, and Z. Bao, "Highly conductive and transparent PEDOT:PSS films with a fluoro-surfactant for stretchable and flexible transparent electrodes," *Advanced functional materials*, vol. 22, no. 2, pp. 421–428, 2012.
- [45] Y. Ding, M. A. Invernale, and G. A. Sotzing, "Conductivity trends of PEDOT:PSS impregnated fabric and the effect of conductivity on electrochromic textile," pp. 1588–1593, Jun 2010. [Online]. Available: <https://www.ncbi.nlm.nih.gov/pubmed/20481442>
- [46] P. Mele, S. Saini, H. Honda, K. Matsumoto, K. Miyazaki, H. Hagino, and A. Ichinose, "Effect of substrate on thermoelectric properties of Al-doped ZnO thin films," *Applied Physics Letters*, vol. 102, no. 25, p. 253903, Jun 24, 2013.
- [47] T. Tsubota, M. Ohtaki, K. Eguchi, and H. Arai, "Thermoelectric properties of Al-doped ZnO as a promising oxide material for high-temperature thermoelectric conversion," *Journal of Materials Chemistry*, vol. 7, no. 1, pp. 85–9, 1997.
- [48] Z. Barasheed, S. S. Kumar, and H. N. Alshareef, "Temperature dependent thermoelectric properties of chemically derived gallium zinc oxide thin films," *Journal of Materials Chemistry C*, vol. 1, no. 26, pp. 4122–4127, 2013.
- [49] K. P. Ong, D. J. Singh, and P. Wu, "Analysis of the thermoelectric properties of n-type ZnO," *Physical Review B*, vol. 83, no. 11, Jan 1, 2011. [Online]. Available: <https://www.osti.gov/biblio/1010579>
- [50] P. Jood, R. J. Mehta, Y. Zhang, G. Peleckis, X. Wang, R. W. Siegel, T. Borca-Tasciuc, S. X. Dou, and G. Ramanath, "Al-doped zinc oxide nanocomposites with enhanced thermoelectric properties," *Nano letters*, vol. 11, no. 10, pp. 4337–4342, Oct 12, 2011. [Online]. Available: <https://www.ncbi.nlm.nih.gov/pubmed/2191044756>
- [51] J. Iqbal, A. Jilani, P. M. Z. Hassan, S. Rafique, R. Jafer, and A. A. Alghamdi, "Al-doped nanostructured ZnO thin films: Effect of substrate temperature on thickness and energy band gap," *Journal of King Saud University - Science*, vol. 28, no. 4, pp. 347–354, Oct 2016. [Online]. Available:

[https://www.openaire.eu/search/publication?articleId=dedup\\_wf\\_001::e75e2152036d019f35bd15db0cf613cf](https://www.openaire.eu/search/publication?articleId=dedup_wf_001::e75e2152036d019f35bd15db0cf613cf)

- [52] T. Tynell and M. Karppinen, "Atomic layer deposition of zno: a review," *Semi-conductor Science and Technology*, vol. 29, no. 4, p. 43001, Apr 1, 2014.
- [53] T. Tynell, H. Yamauchi, M. Karppinen, R. Okazaki, and I. Terasaki, "Atomiclayer deposition of al-doped zno thin films," *Journal of Vacuum Science Tech-nology A Vacuum, Surfaces, and Films*, vol. 31, no. 1, p. 01A109, 2013.
- [54] Lund, N. M. van der Velden, N.-K. Persson, M. M. Hamed, and C. Mueller, "Electrically conducting fibres for e-textiles: An open playground for conjugatedpolymers and carbon nanomaterials," *Materials Science and Engineering: R:Reports*, vol. 126, pp. 1–29, 2018.
- [55] V. Leonov, "Thermoelectric energy harvesting of human body heat for wearablesensors," *IEEE Sensors Journal*, vol. 13, no. 6, pp. 2284–2291, Jun 2013.[Online]. Available: <https://ieeexplore.ieee.org/document/6479224>
- [56] J. Karttunen, L. Sarnes, R. Townsend, J. Mikkonen, and M. Karppinen, "Flexible thermoelectric zno–organic superlattices on cotton textile substrates byald/mld," *Advanced Electronic Materials*, vol. 3, no. 6, p. n/a, Jun 2017. [Online].Available: <https://onlinelibrary.wiley.com/doi/abs/10.1002/aelm.201600459>
- [57] J. A. Lee, A. E. Aliev, J. S. Bykova, M. J. de Andrade, D. Kim, H. J.Sim, X. Lepró, A. A. Zakhidov, J. Lee, and G. M. Spinks, "Woven-yarnthermoelectric textiles," *Advanced Materials*, vol. 28, no. 25, pp. 5038–5044, 2016.
- [58] L. Sarnes, "Termosähköisten oksidimateriaalien atomikerroskasvatus tekstiileille;atomic layer deposition of thermoelectric oxide materials on textiles," Ph.D. 57dissertation, -12-15 2015. [Online] . Available: [http://urn.fi/URN:NBN:fi:aalto-201512165638\[urn\]](http://urn.fi/URN:NBN:fi:aalto-201512165638[urn])
- [59] J. D. Ryan, D. A. Mengistie, R. Gabrielsson, A. Lund, and C. Müller, "Machine-washable pedot:pss dyed silk yarns for electronic textiles," *ACSApplied materials & interfaces*, vol. 9, no. 10, pp. 9045–9050, Mar 15, 2017.[Online]. Available: <https://www.ncbi.nlm.nih.gov/pubmed/28245105>

- [60] J. S. Jur, W. J. S. III, C. J. Oldham, and G. N. Parsons, "Atomic layer deposition of conductive coatings on cotton, paper, and synthetic fibers: conductivity analysis and functional chemical sensing using "all-fiber" capacitors," *Advanced functional materials*, vol. 21, no. 11, pp. 1993–2002, 2011.
- [61] T. Stöcker, A. Köhler, and R. Moos, "Why does the electrical conductivity in PEDOT:PSS decrease with PSS content? a study combining thermoelectric measurements with impedance spectroscopy", *Journal of Polymer Science Part B: Polymer Physics*, vol 50, no 14, pp. 976-983, Jul 15, 2012.